Analytical and semi-analytical approaches to modeling transient fluid-structure interaction

Serguei Iakovlev

Department of Engineering Mathematics and Internetworking, Dalhousie University, Canada

Department of Structural Mechanics, University of Pavia, Italy

Some examples of systems where
fluid-structure interaction is of importance

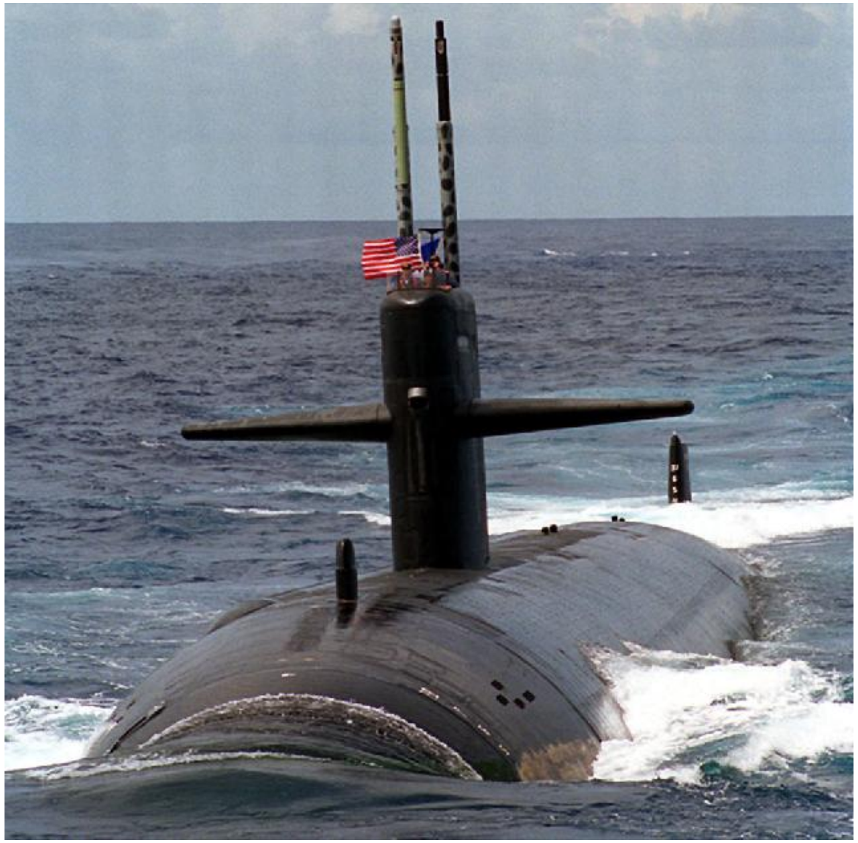


©AMEC Border Wind

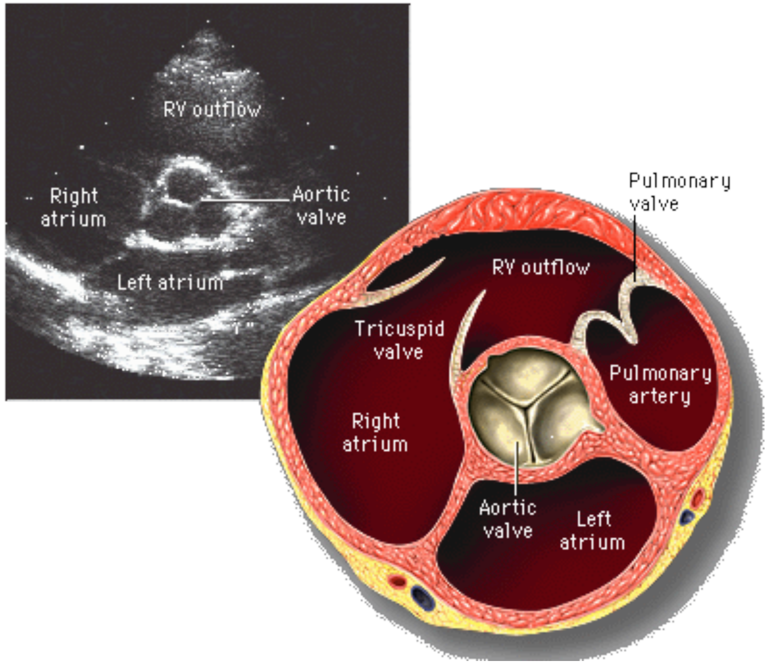
RV outflow
Right atrium
Aortic valve
Left atrium
Pulmonary valve
RV outflow
Tricuspid valve
Pulmonary artery
Right atrium
Aortic valve
Left atrium

Brief history of shell-shock interaction analysis

- 1950s: analytical solutions, structural analysis mostly confined to individual modes
- 1960s: analytical solutions, two-dimensional structural analysis, surface pressure, various asymptotics + experiments
- 1970s: analytical solutions, first attempts at three-dimensional structural analysis, surface pressure + experiments
- 1980s: major shift to numerical solutions, both structural analysis and analysis of pressure fields + more advanced experiments
- 1990s: major advancement of numerical methods + experimental images of unparalleled quality
- Today: “golden age” of numerical methods

Part I:

External loading on a submerged but empty cylindrical shell

(2D analysis)

Inspired by Geers (1969) who first introduced the combination of the Laplace transform and separation of variables to compute the surface (1D) distribution of the pressure and displacements during the response of a cylindrical shell to a shock wave

Geometry of the problem

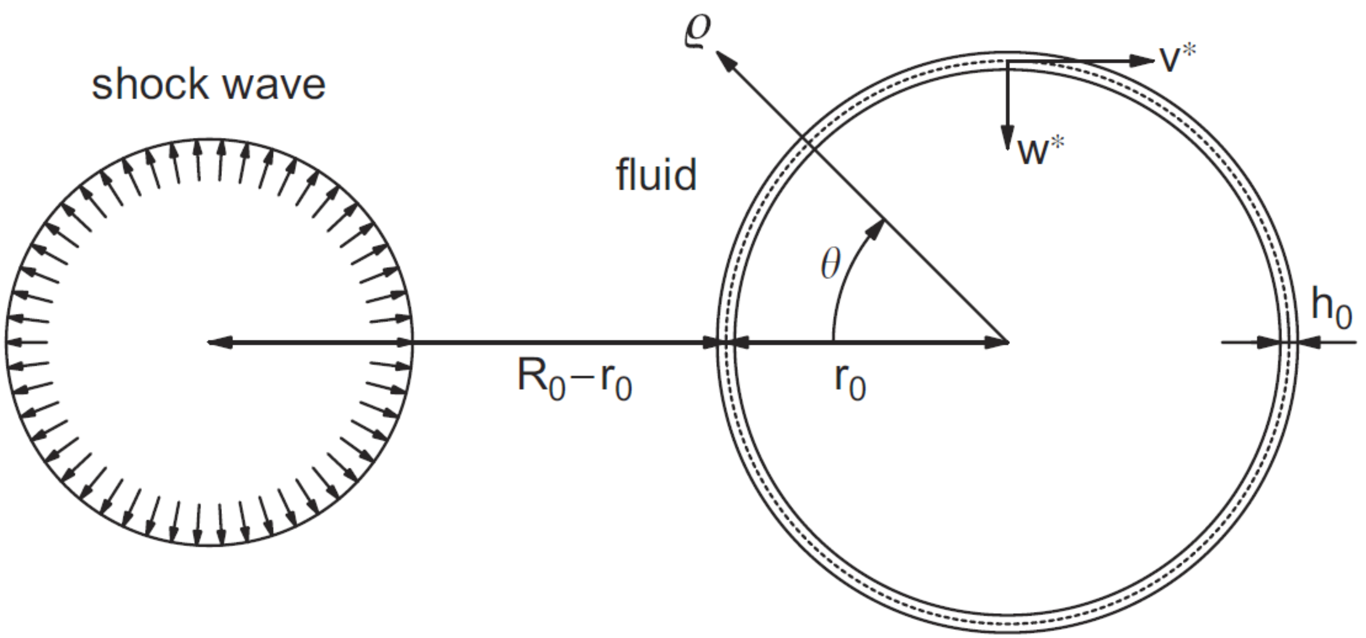

$$r = \varrho r_0^{-1}$$

$$v = v^* r_0^{-1}$$

$$w = w^* r_0^{-1}$$

$$t = \tau c_f r_0^{-1}$$

Boundary value problem

$$\nabla^2 \hat{\phi} = \frac{\partial^2 \hat{\phi}}{\partial t^2} \qquad \hat{\phi} = \hat{\phi}_0 + \hat{\phi}_d + \hat{\phi}_r$$

$$\frac{\partial^2 v}{\partial \theta^2} - \frac{\partial w}{\partial \theta} + k_0^2 \left(\frac{\partial^3 w}{\partial \theta^3} + \frac{\partial^2 v}{\partial \theta^2} \right) = \frac{1}{\hat{c}_s^2} \frac{\partial^2 v}{\partial t^2},$$

$$w - \frac{\partial v}{\partial \theta} + k_0^2 \left(\frac{\partial^4 w}{\partial \theta^4} + \frac{\partial^3 v}{\partial \theta^3} \right) = \hat{\chi} \hat{p}|_{r=1} - \frac{1}{\hat{c}_s^2} \frac{\partial^2 w}{\partial t^2}$$

$$\left. \frac{\partial \hat{\phi}_r}{\partial r} \right|_{r=1} = -\frac{\partial w}{\partial t} \qquad \left. \frac{\partial \hat{\phi}_d}{\partial r} \right|_{r=1} = - \left. \frac{\partial \hat{\phi}_0}{\partial r} \right|_{r=1}$$

Solution – fluid dynamics

Laplace transform in time

$$\frac{\partial^2 \hat{\Phi}_e}{\partial r^2} + \frac{1}{r}\frac{\partial \hat{\Phi}_e}{\partial r} + \frac{1}{r^2}\frac{\partial^2 \hat{\Phi}_e}{\partial \theta^2} - s^2 \hat{\Phi}_e = 0$$

Separation of variables in space

$$\hat{\Phi} = \{F_n \mathrm{I}_n(rs) + G_n \mathrm{K}_n(rs)\} \cos n\theta, \quad n = 0, 1, \ldots,$$

Solution – fluid dynamics

$$\hat{\Phi} = A_n \mathrm{K}_n(rs) \cos n\theta, \quad n = 0, 1, \ldots$$

$$\hat{\Phi}_n^d = B_n \Xi_n^e \cos n\theta$$

$$\hat{\Phi}_n^r = s W_n \Xi_n^e \cos n\theta$$

$$\Xi_n^e(r, s) = -\frac{\mathrm{K}_n(rs)}{s\mathrm{K}_n'(s)}$$

$$\hat{p}_n^d = -\frac{1}{\sqrt{r}}\, b_n(t) - \int_0^t b_n(\eta)\, \frac{\mathrm{d}\xi_n^e}{\mathrm{d}\eta}(r, t-\eta)\, \mathrm{d}\eta$$

$$\hat{p}_n^r = -\int_0^t \frac{\mathrm{d}^2 w_n(\eta)}{\mathrm{d}\eta^2}\, \xi_n^e(r, t-\eta)\, \mathrm{d}\eta$$

$$\hat{p} = \sum_{n=0}^{\infty} \hat{p}_n \cos n\theta$$

Solution – structural dynamics

$$v = \sum_{n=0}^{\infty} v_n \sin n\theta, \quad w = \sum_{n=0}^{\infty} w_n \cos n\theta$$

$$\gamma^2 \frac{\mathrm{d}^2 v_n}{dt^2} + c_n^{11} v_n + c_n^{12} w_n = 0,$$
$$\gamma^2 \frac{\mathrm{d}^2 w_n}{dt^2} + c_n^{21} v_n + c_n^{22} w_n = \hat{\chi} \left\{ \hat{p}_n^0 + \hat{p}_n^d - \int_0^t \frac{\mathrm{d}^2 w_n(\eta)}{\mathrm{d}\eta^2} \, \xi_n^e(r, t-\eta) \, \mathrm{d}\eta \right\} \Bigg|_{r=1}$$

$$c_n^{11} = n^2 + k_0^2 n^2, \quad c_n^{12} = c_n^{21} = -n - k_0^2 n^3, \quad c_{mn}^{22} = 1 + k_0^2 n^4, \quad \gamma = \hat{c}_s^{-1}$$

[finite difference approximation is used to solve the system]

Solution – structural dynamics

$$v_n^{i+1} = 2v_n^i - v_n^{i-1} - \frac{h^2}{\gamma^2}\{c_n^{11}v_n^i + c_n^{12}w_n^i\},$$

$$w_n^{i+1} = 2w_n^i - w_n^{i-1} + \frac{2h^2}{\delta_h h + 2\gamma^2}\{\delta_h(p_n^i - hJ_n^i) - c_n^{21}v_n^i - c_n^{22}w_n^i\}$$

$$J_n^i = \sum_{j=1}^{i-1}\{w_n^{j+1} - 2w_n^j + w_n^{j-1}\}\,h^{-2}\,\psi_n^{i-j}$$

Convergence of the finite-difference scheme for the structural components

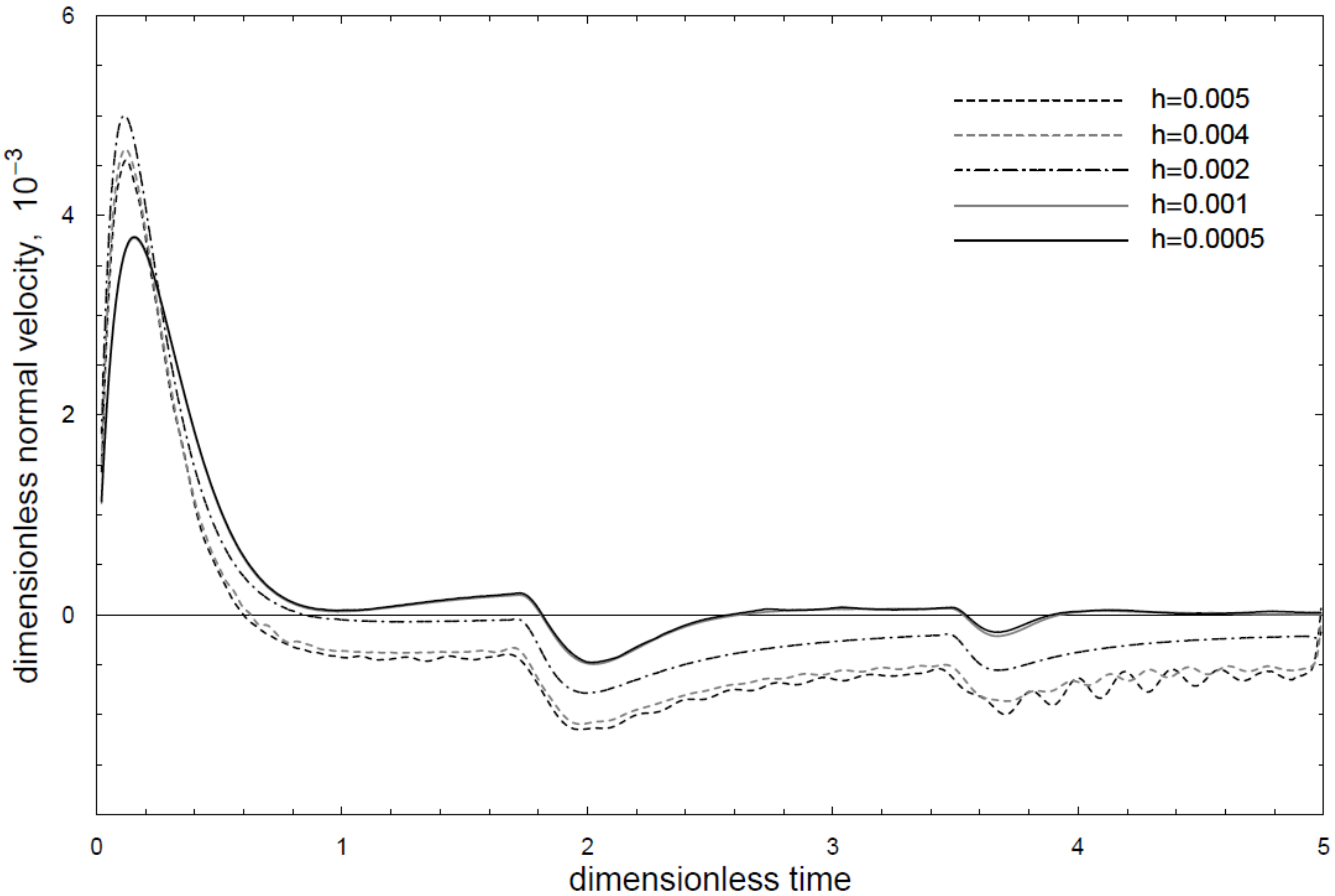

Response functions – analytical inversion

$$\Xi_n^e(r,s) = -\frac{\mathrm{K}_n(rs)}{s\mathrm{K}_n'(s)}$$

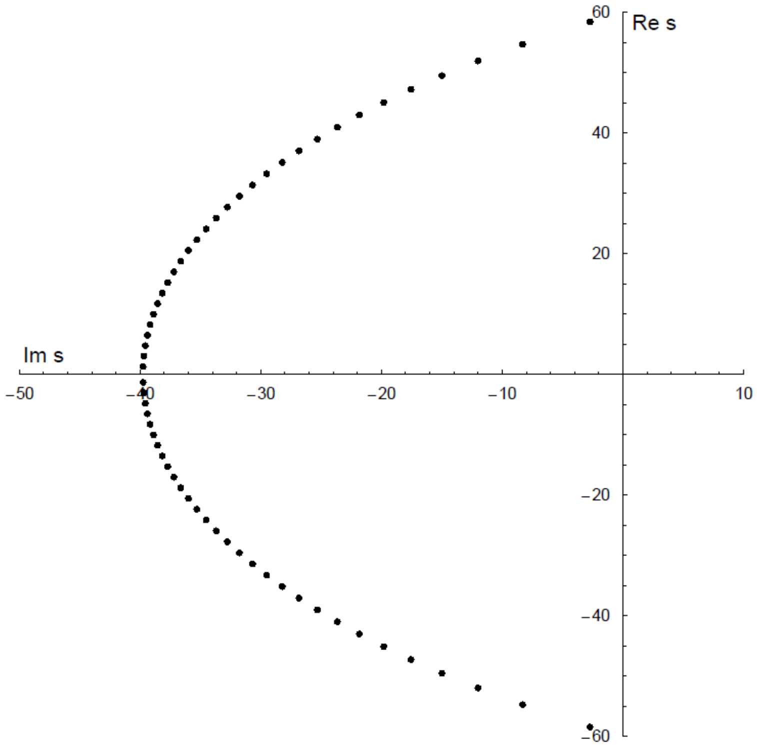

$$\Xi_n^e(r,s) \sim \frac{1}{s\sqrt{r}}\,\mathrm{e}^{s(1-r)}, \quad |s| \gg 1$$

$$\Xi_n^e(r,s) \sim \frac{1}{s\sqrt{r}}\,\mathrm{e}^{s(1-r)}, \quad |s| \gg 1$$

$$\Xi_n^*(r,s) = \Xi_n^e(r,s)\,\mathrm{e}^{s(r-1)} = -\frac{\mathrm{K}_n(rs)}{s\mathrm{K}_n'(s)}\,\mathrm{e}^{s(r-1)}$$

$$\Xi_n^*(r,t) \sim \frac{1}{s\sqrt{r}}, \quad |s| \gg 1$$

$$\xi_n^e(r,t) = \xi_n^*(r,t-r+1)\mathrm{H}(t-r+1)$$

Mellin's integral

$$\xi_n^*(r,t) = \frac{1}{2\pi \mathrm{i}} \int_{\epsilon-\mathrm{i}\infty}^{\epsilon+\mathrm{i}\infty} \Xi_n^*(r,s)\mathrm{e}^{st}\mathrm{d}s$$

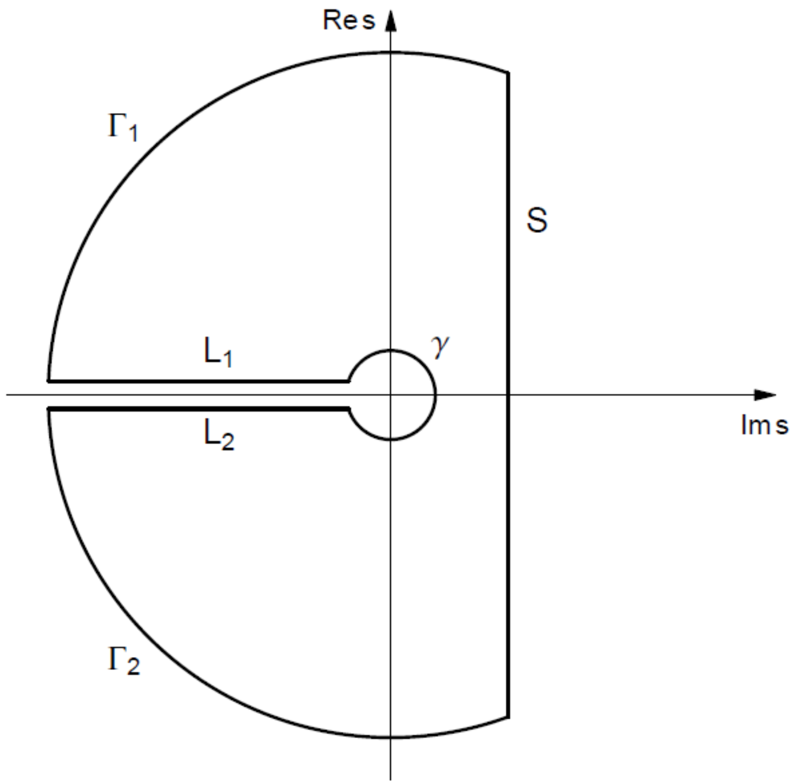

$$\int_\Gamma [*] = \int_\gamma [*] + \int_{\Gamma_1} [*] + \int_{\Gamma_2} [*] + \int_{L_1} [*] + \int_{L_2} [*] + \int_S [*] = 2\pi \mathrm{i} \sum_{k=1}^{N} R_k^n$$

$$\xi_n^*(r,t) = -\sum_{k=1}^{N} \frac{\mathrm{K}_n(r s_k^n)}{\mathrm{K}_n(s_k^n)} \frac{s_k^n}{(s_k^n)^2 + n^2} \, \mathrm{e}^{s_k^n t} \; + \\ (-1)^n \int_0^\infty \frac{\left\{ \mathrm{I}_n(r\eta)\tilde{\mathrm{K}}_n(\eta) + \mathrm{K}_n(r\eta)\tilde{\mathrm{I}}_n(\eta) \right\}}{\eta \left\{ \tilde{\mathrm{K}}_n^2(\eta) + \pi^2 \tilde{\mathrm{I}}_n^2(\eta) \right\}} \, \mathrm{e}^{-\alpha\eta} \, \mathrm{d}\eta$$

$$\xi_0^*(r,t) = \int_0^\infty \frac{\{ \mathrm{I}_0(r\eta)\mathrm{K}_1(\eta) + \mathrm{K}_0(r\eta)\mathrm{I}_1(\eta) \}}{\eta \{ \mathrm{K}_1^2(\eta) + \pi^2 \mathrm{I}_1^2(\eta) \}} \, \mathrm{e}^{-\alpha\eta} \, \mathrm{d}\eta$$

$$\tilde{\mathrm{K}}_n(\eta) = \mathrm{K}_{n-1}(\eta) + \frac{n}{\eta} \mathrm{K}_n(\eta) \qquad \tilde{\mathrm{I}}_n(\eta) = \mathrm{I}_{n-1}(\eta) - \frac{n}{\eta} \mathrm{I}_n(\eta)$$

Response functions – numerical inversion
[based on the idea proposed by Dubner and Abate (1968)]

$$\xi_n^* = \frac{2\mathrm{e}^{at}}{\pi} \int_0^\infty \mathrm{Re}\left\{\Xi_n^*(r, s)\right\} \cos \omega t \, \mathrm{d}\omega$$

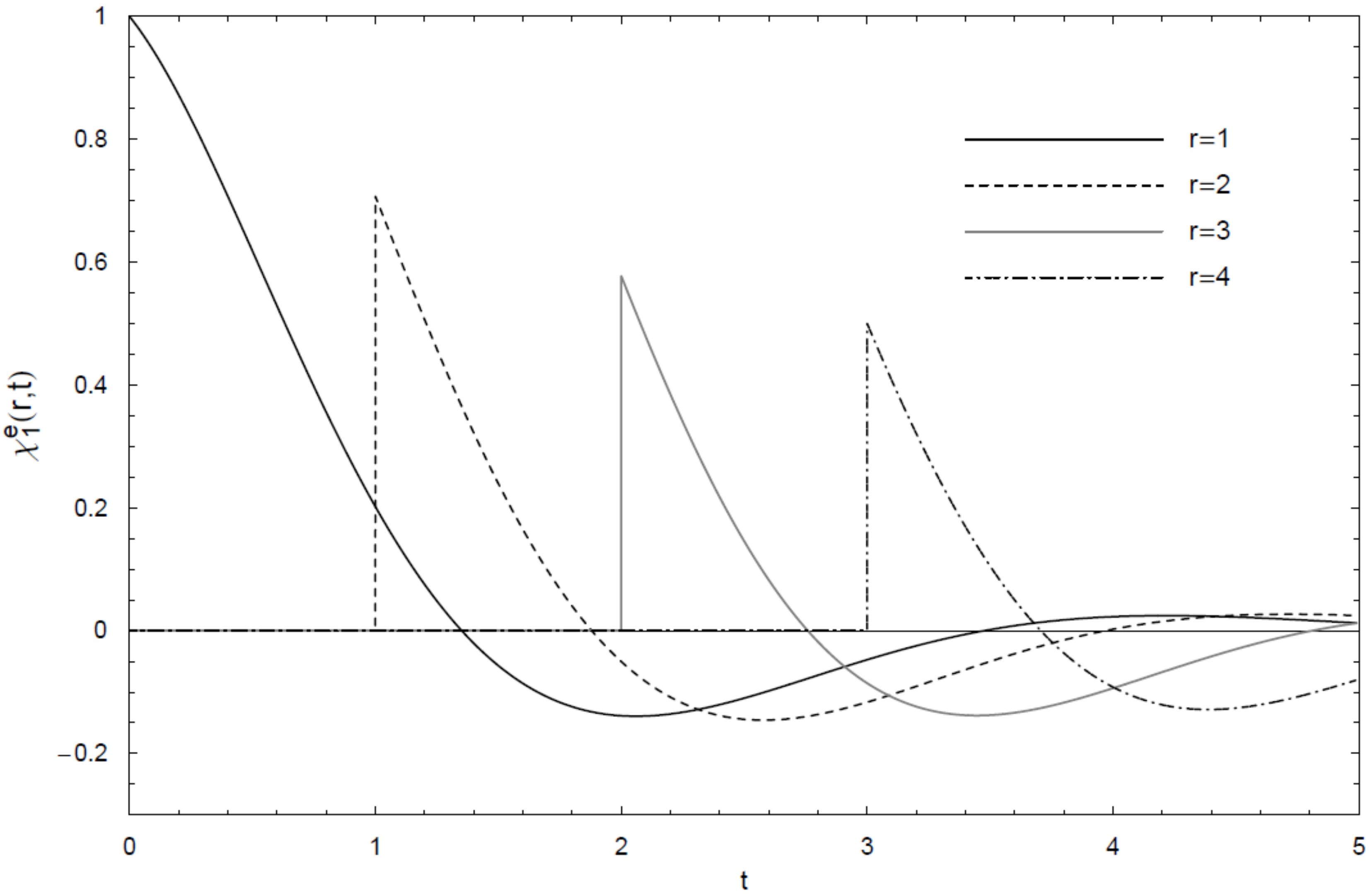

1
0.8
0.6
0.4
0.2
0
−0.2
0
1
2
3
4
5
t
$\chi_1^e(r,t)$
r=1
r=2
r=3
r=4

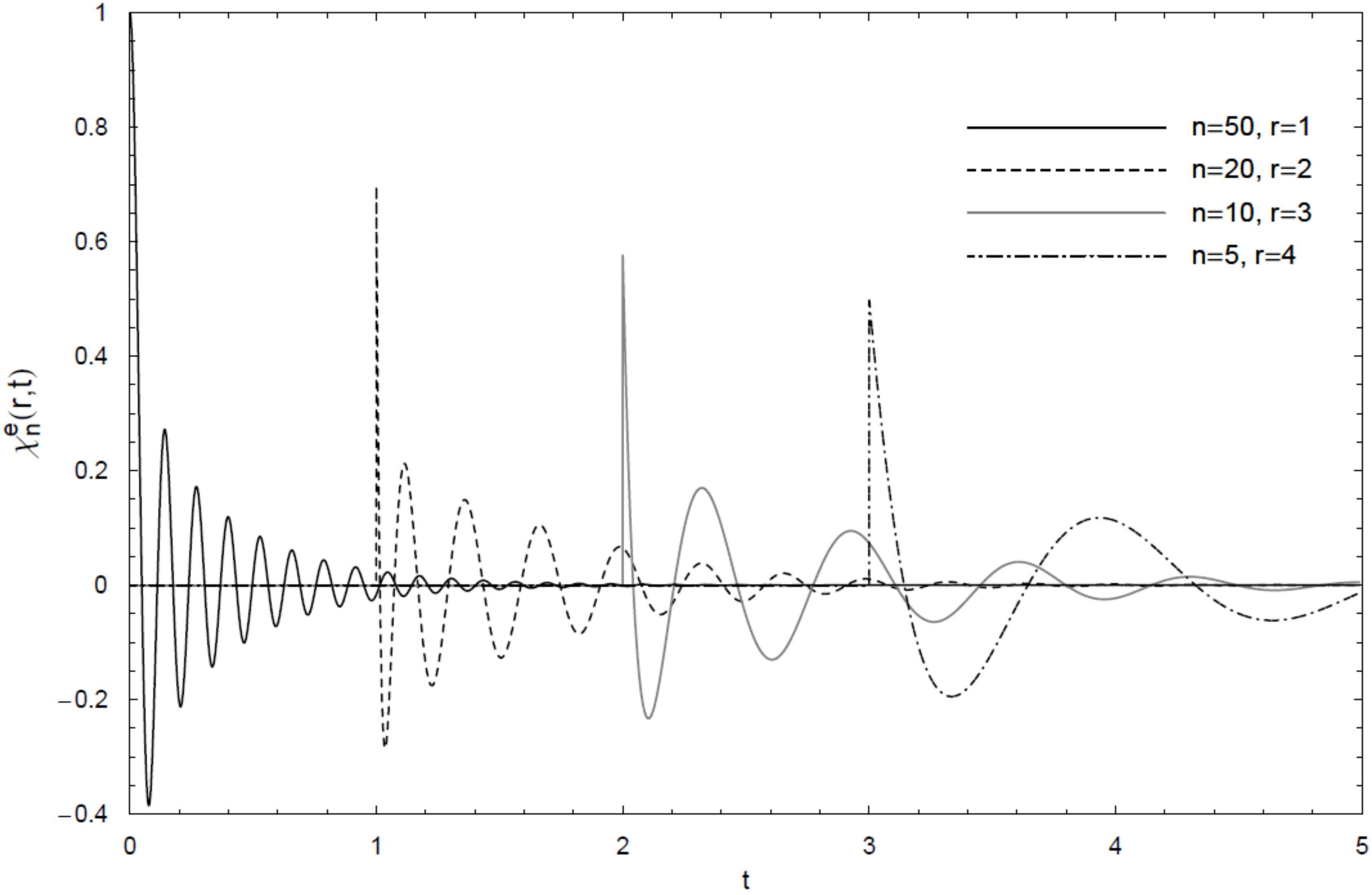

n=50, r=1
n=20, r=2
n=10, r=3
n=5, r=4
$\chi_n^e(r,t)$
t
1
0.8
0.6
0.4
0.2
0
−0.2
−0.4
0
1
2
3
4
5

Diffraction pressure only (rigid cylinder, elasticity "switched off")

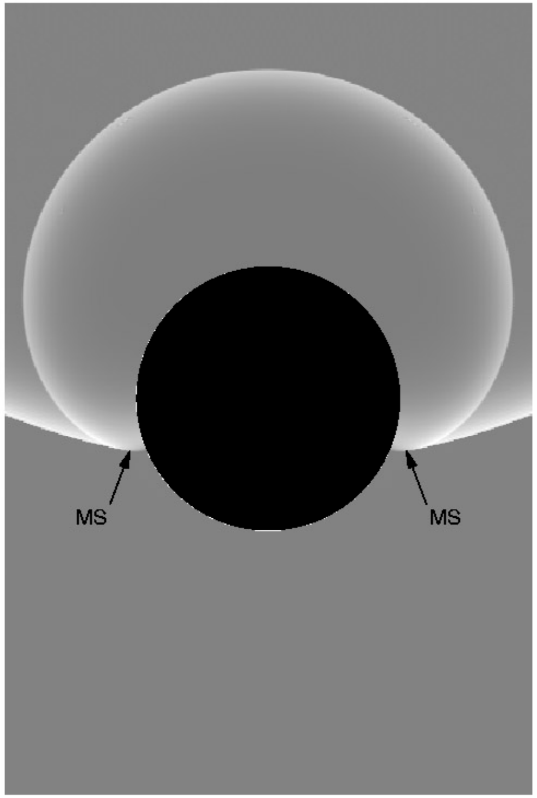

Numerically simulated pressure pattern

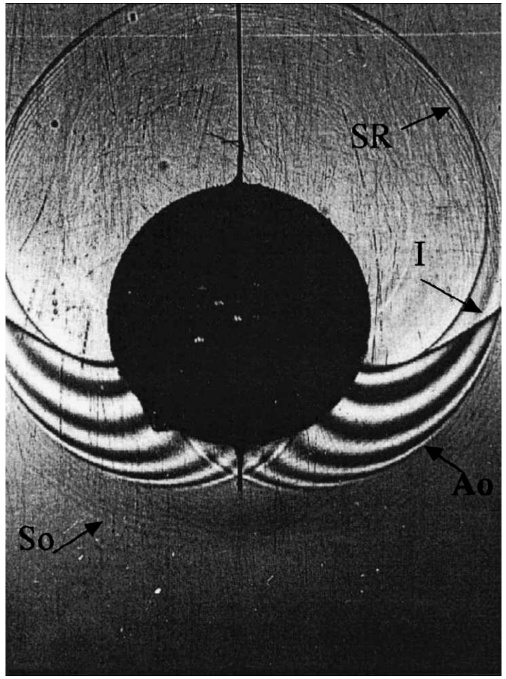

Ahyi, A. C., Pernod, P., Gatti, O., Latard, V., Merlen, A. and Uberall, H. Experimental demonstration of the pseudo-Rayleigh A0 wave. *Journal of the Acoustical Society of America* 104, 1998, 2727-2732. © American Institute of Physics.

Convergence of the diffraction pressure

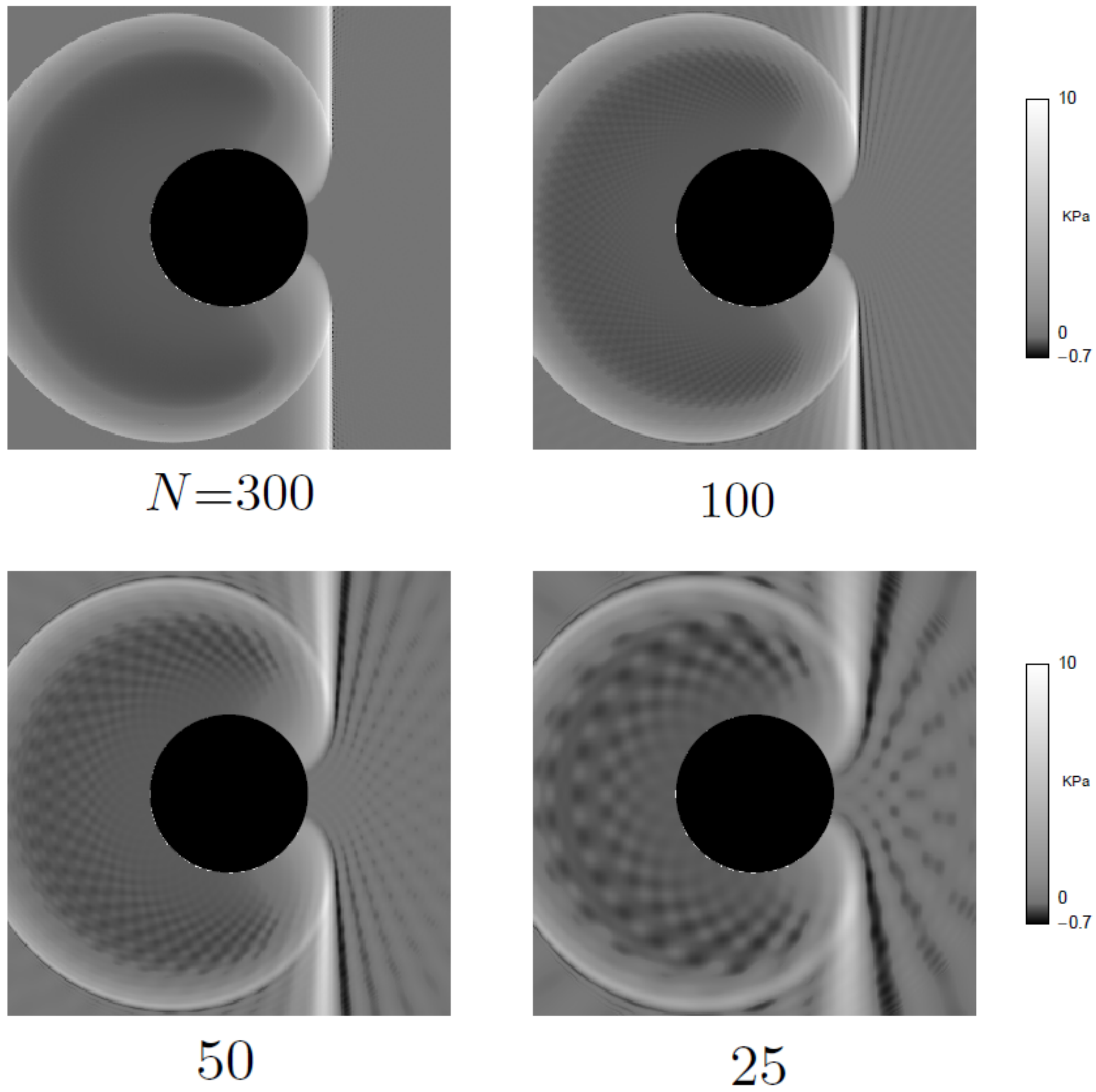

Complete diffraction-radiation analysis (elasticity “switched on”)

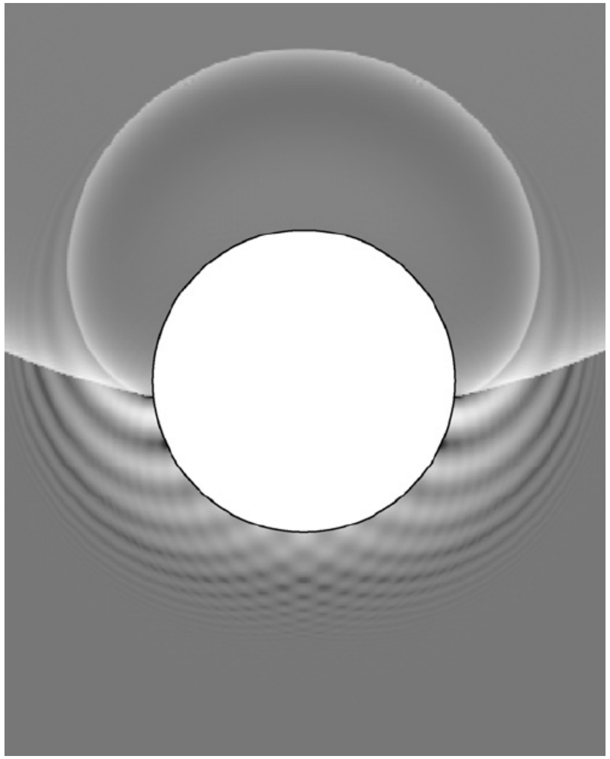

Numerically simulated pressure pattern

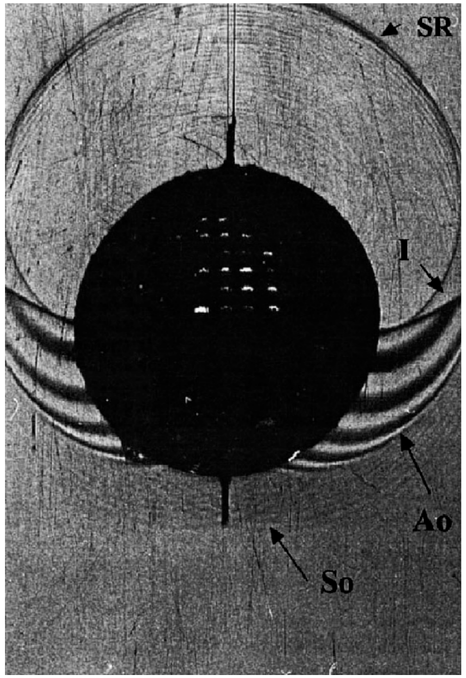

Ahyi, A. C., Pernod, P., Gatti, O., Latard, V., Merlen, A. and Uberall, H. Experimental demonstration of the pseudo-Rayleigh A0 wave. *Journal of the Acoustical Society of America* 104, 1998, 2727-2732. © American Institute of Physics.

Part II:

External loading on a submerged *fluid-filled* cylindrical shell

(2D analysis)

Inspired by Geers (1969) and a need for modeling shock loading on underwater oil pipelines and storage tanks

Geometry of the problem

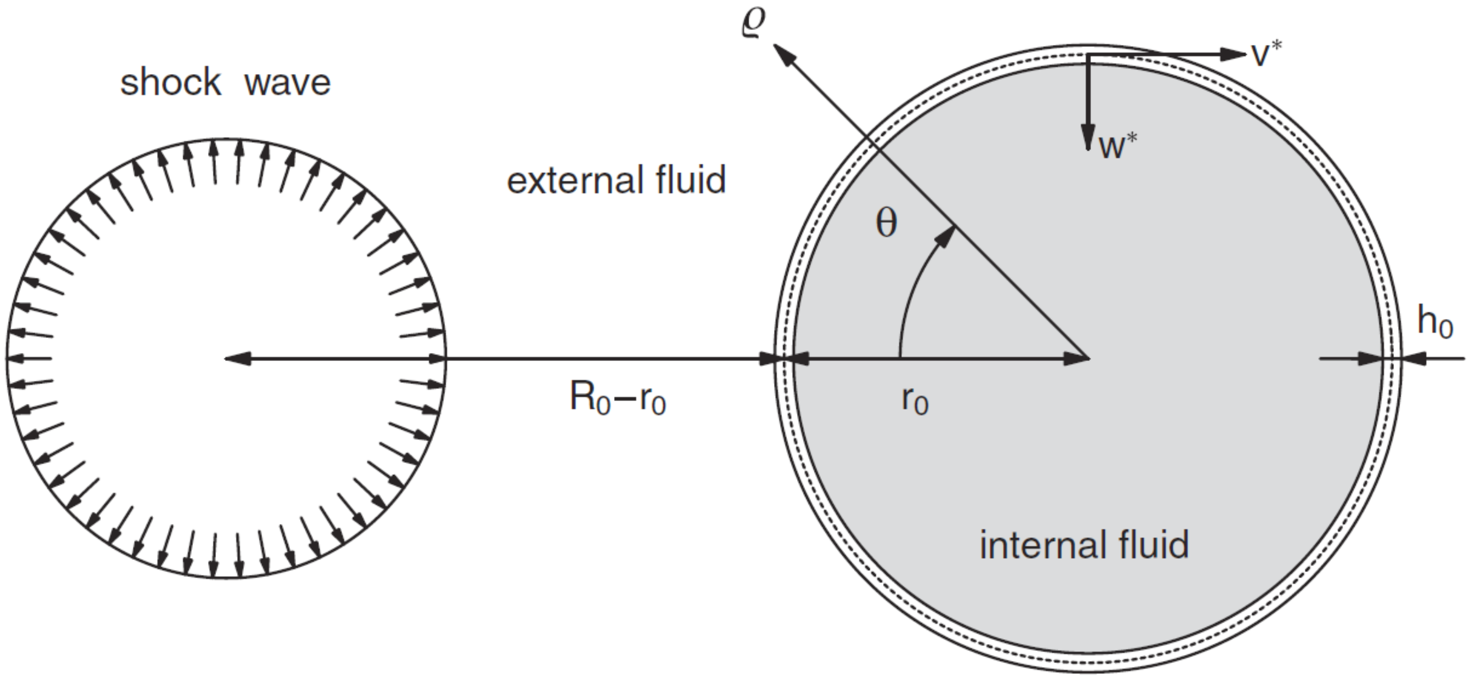

$$\hat{\phi} = \hat{\phi}_0 + \hat{\phi}_d + \hat{\phi}_r^e - \hat{\phi}_r^i$$

Solution – fluid dynamics

$$\hat{p}_n^d = -b_n(t) - \int_0^t b_n(\eta)\,\frac{\mathrm{d}\psi_n^e}{\mathrm{d}\eta}(t-\eta)\,\mathrm{d}\eta$$

$$\hat{p}_n^{r,e} = -\int_0^t \frac{\mathrm{d}^2 w_n(\eta)}{\mathrm{d}\eta^2}\,\psi_n^e(t-\eta)\,\mathrm{d}\eta$$

$$\hat{p}_n^{r,i} = \int_0^t \frac{\mathrm{d}^2 w_n(\eta)}{\mathrm{d}\eta^2}\,\xi_n^i(r,t-\eta)\,\mathrm{d}\eta$$

Internal response functions – analytical inversion

$$\Xi_n^i(r, s) = \frac{\mathrm{I}_n(rs)}{s\mathrm{I}_n'(s)}$$

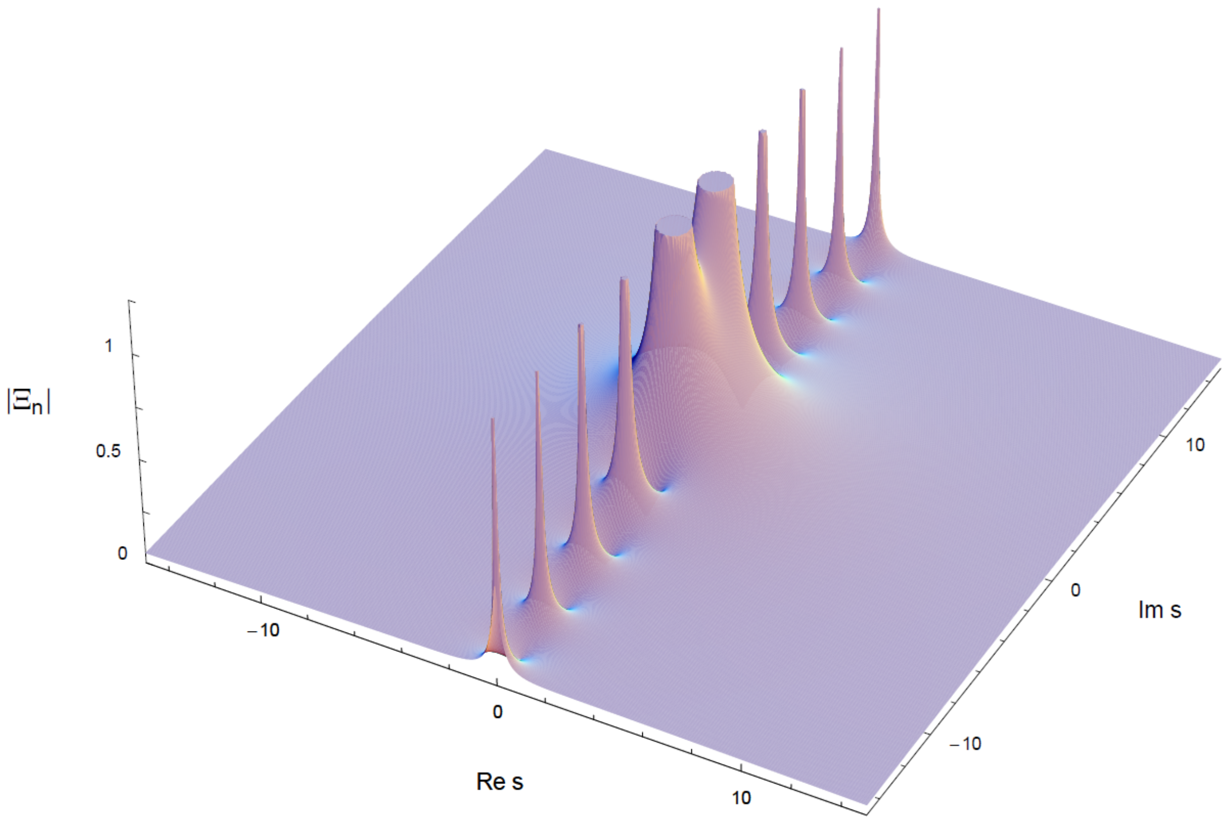

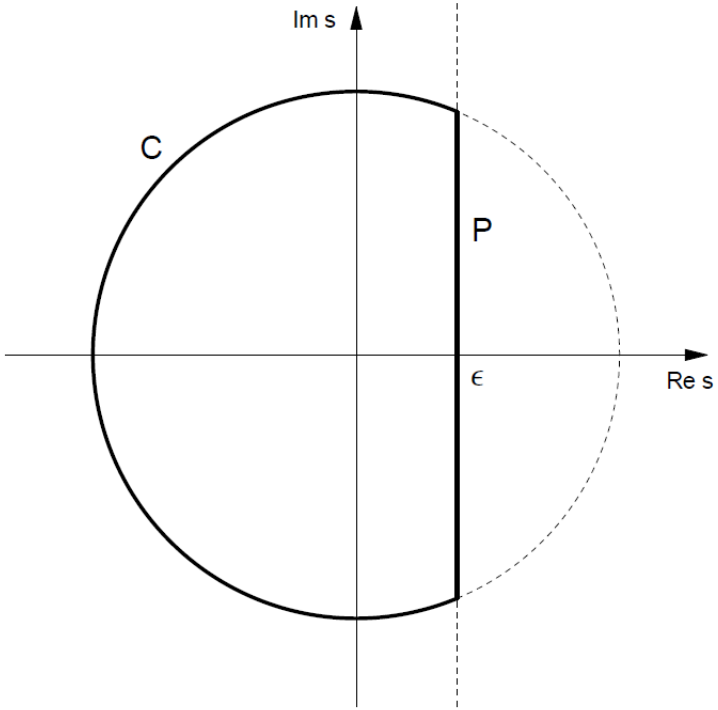

$$s = R\mathrm{e}^{i\phi} \qquad |\Xi_n| \sim \frac{1}{R}\chi(r, R, \phi)$$

$$\chi(r, R, \phi) = \left\{ \frac{\mathrm{e}^{2rR\cos\phi} + \mathrm{e}^{-2rR\cos\phi} + 2\sin(2rR\sin\phi)}{\mathrm{e}^{2R\cos\phi} + \mathrm{e}^{-2R\cos\phi} - 2\sin(2R\sin\phi)} \right\}^{\frac{1}{2}}$$

$$R_k = \pi k, \quad k = 1, 2, \ldots$$

$$\xi_0(r,t) = 2t + 2\sum_{k=1}^{\infty} \frac{\mathrm{J}_0(r\omega_k^0)}{\mathrm{J}_0(\omega_k^0)}\,\frac{1}{\omega_k^0}\sin(\omega_k^0 t)$$

$$\xi_n(r,t) = 2\sum_{k=1}^{\infty} \frac{\mathrm{J}_n(r\omega_k^n)}{\mathrm{J}_n(\omega_k^n)}\,\frac{\omega_k^n}{\{(\omega_k^n)^2 - n^2\}}\sin(\omega_k^n t), \quad n \geq 1$$

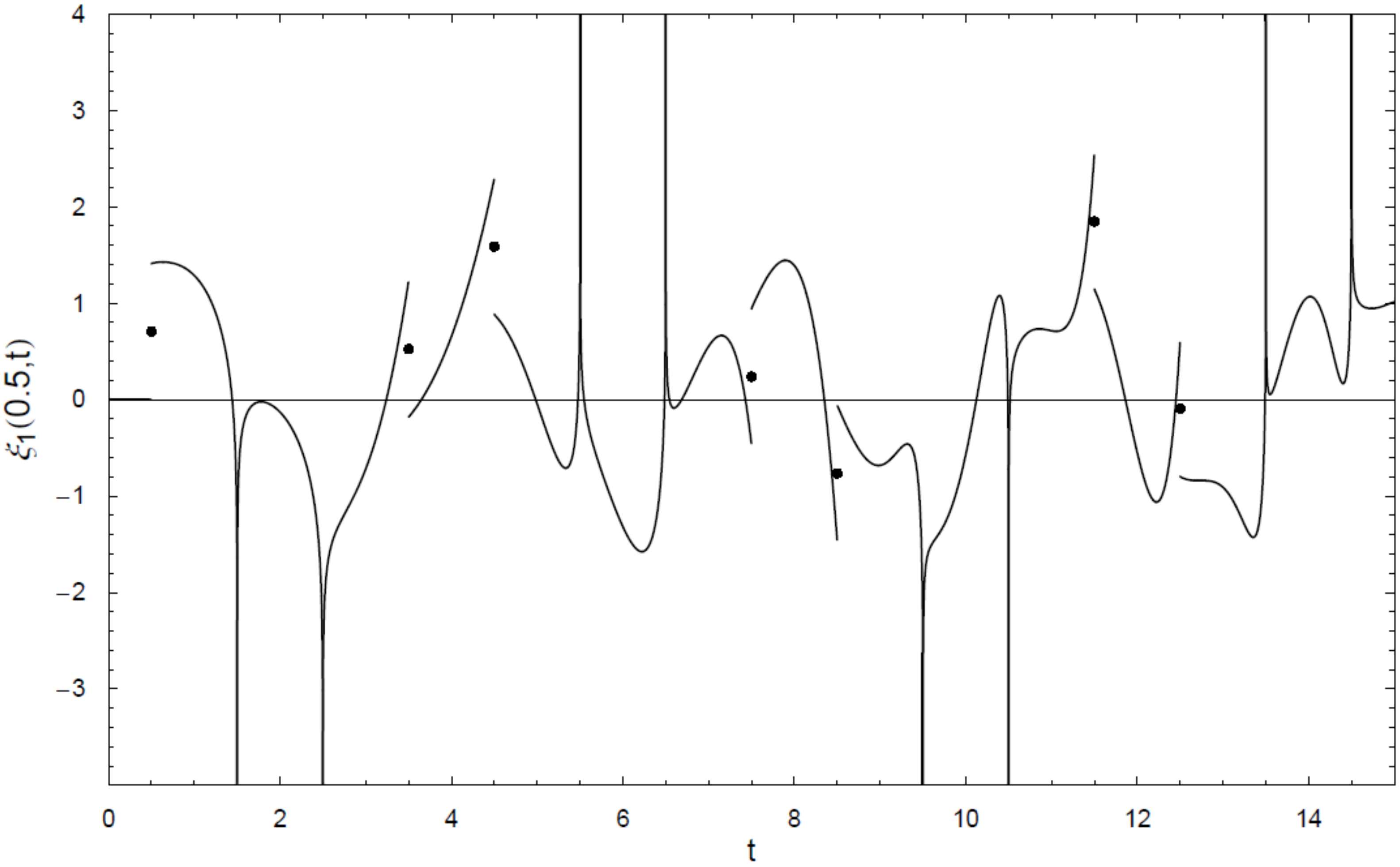

4
3
2
1
0
−1
−2
−3
$\xi_1(0.5,t)$
0
2
4
6
8
10
12
14
t

Singularities

$$\gamma_k(n,r,t) = 2\,\alpha_k^n(r)\,\frac{\omega_k^n}{((\omega_k^n)^2 - n^2)}\sin(\omega_k^n t) \qquad \alpha_k^n(r) = \frac{\mathrm{J}_n(r\omega_k^n)}{\mathrm{J}_n(\omega_k^n)}$$

$$\gamma_k = \frac{\cos(\beta_k^n(r-1))\sin(\beta_k^n t)}{\sqrt{r}\,\pi k} + O\left(\frac{1}{k^2}\right), \quad k \gg 1$$

$$2\sum_{k=N}^{\infty}\frac{\mathrm{J}_n(r\omega_k^n)}{\mathrm{J}_n(\omega_k^n)}\,\frac{\omega_k^n}{\{(\omega_k^n)^2 - n^2\}}\sin(\omega_k^n t) = I_1 + I_2$$

$$I_1 = \frac{2}{\pi\sqrt{r}}\sum_{k=N}^{\infty}\frac{\cos(\beta_k^n(r-1))\sin(\beta_k^n t)}{k} \qquad I_2 = \sum_{k=N}^{\infty} O\left(\frac{1}{k^2}\right)$$

$$I_1 = G_1 + G_2$$

$$G_1 = \frac{1}{\pi\sqrt{r}} \sum_{k=N}^{\infty} \frac{\sin(\beta_k^n(t+r-1))}{k} \qquad t_1^s = 2(2j+1) - r + 1, \quad j = 0, 1, \ldots$$

$$G_2 = \frac{1}{\pi\sqrt{r}} \sum_{k=N}^{\infty} \frac{\sin(\beta_k^n(t-r+1))}{k} \qquad t_2^s = 2(2j+1) + r - 1, \quad j = 0, 1, \ldots$$

$$\begin{array}{llllllll} t: & 1+r & 3-r & 5+r & 7-r & 9+r & 11-r & \ldots \\ \xi_n(r,t): & -\infty & -\infty & \infty & \infty & -\infty & -\infty & \ldots \end{array}$$

$$\begin{array}{llllllll} t: & 1+r & 3-r & 5+r & 7-r & 9+r & 11-r & \ldots \\ \xi_n(r,t): & \infty & \infty & -\infty & -\infty & \infty & \infty & \ldots \end{array}$$

Why worry so much about the singularities?

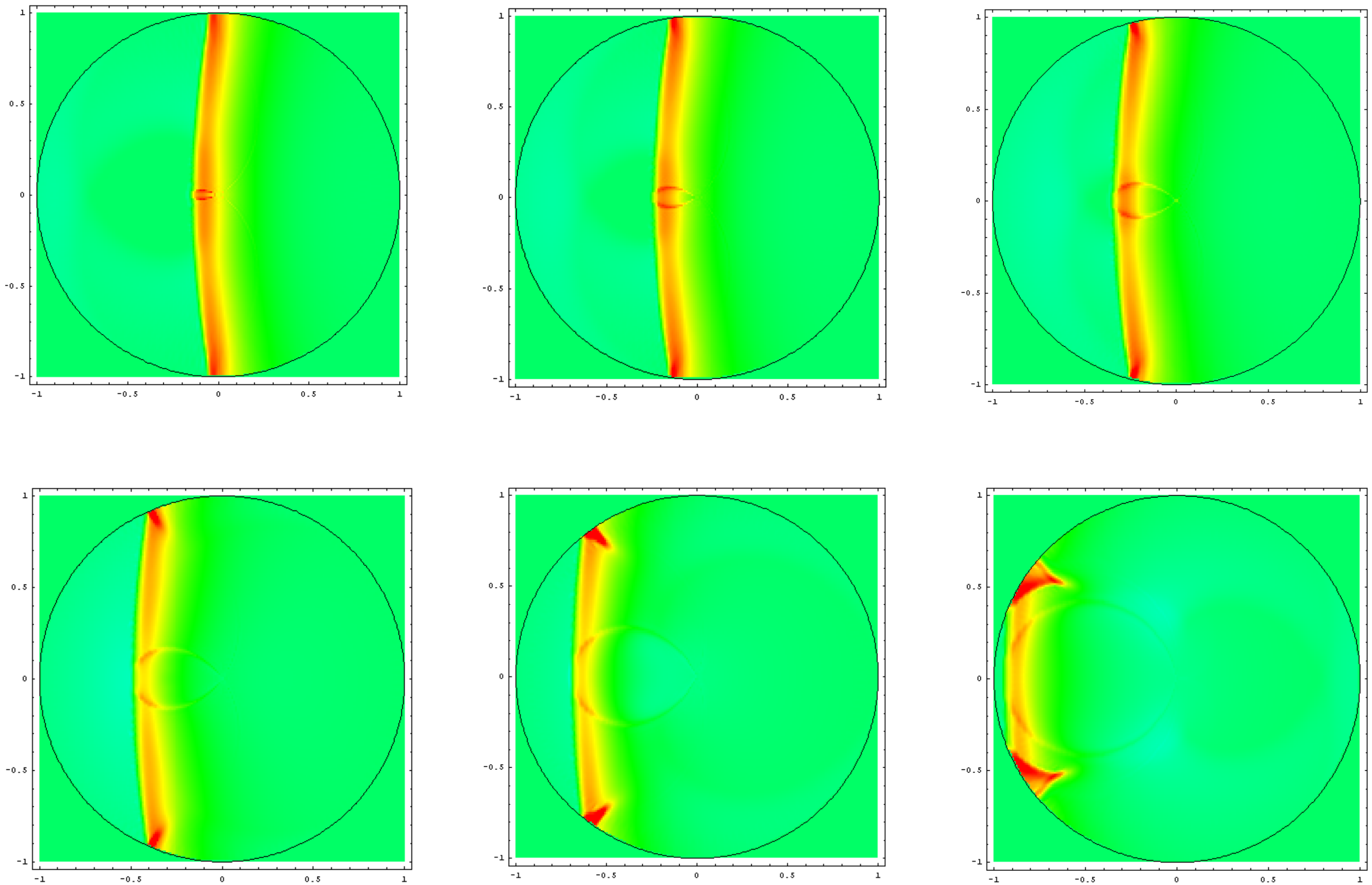

Discontinuities

$$I_1 = G_1 + G_2$$

$$t_1^f = 4m - r + 1, \quad m = 0, 1, \dots$$

$$t_2^f = 4(m+1) + r - 1, \quad m = 0, 1, \dots$$

$$G_1\big|_{t=4m-r+1\pm\delta} = \pm \frac{(-1)^m}{\pi\sqrt{r}} Q(\delta, N)$$

$$Q(\delta, N) = \frac{\mathrm{e}^{i\delta\pi\left(N+\frac{n}{2}-\frac{3}{4}\right)}}{2i}\Phi(\mathrm{e}^{i\delta\pi}, 1, N) - \frac{\mathrm{e}^{-i\delta\pi\left(N+\frac{n}{2}-\frac{3}{4}\right)}}{2i}\Phi(\mathrm{e}^{-i\delta\pi}, 1, N)$$

$$Q(\delta, N) \to \frac{\pi}{2} \text{ as } \delta \to 0$$

$$\lim_{t\to(4m-r+1)^-} G_1 = -\frac{(-1)^m}{2\sqrt{r}} \qquad \lim_{t\to(4m-r+1)^+} G_1 = \frac{(-1)^m}{2\sqrt{r}}$$

$$\lim_{t\to(4(m+1)+r-1)^-} G_2 = \frac{(-1)^m}{2\sqrt{r}} \qquad \lim_{t\to(4(m+1)+r-1)^+} G_2 = -\frac{(-1)^m}{2\sqrt{r}}$$

$$\begin{array}{llllllllll} t_f: & 1-r & 3+r & 5-r & 7+r & 9-r & 11+r & 13-r & \dots \\ L: & -\frac{1}{\sqrt{r}} & \frac{1}{\sqrt{r}} & \frac{1}{\sqrt{r}} & -\frac{1}{\sqrt{r}} & -\frac{1}{\sqrt{r}} & \frac{1}{\sqrt{r}} & \frac{1}{\sqrt{r}} & \dots \end{array}$$

$$\xi_n(r,t)|_{t=t_f} = \frac{1}{2}\left\{\lim_{t\to t_f^-} \xi_n(r,t) + \lim_{t\to t_f^+} \xi_n(r,t)\right\}$$

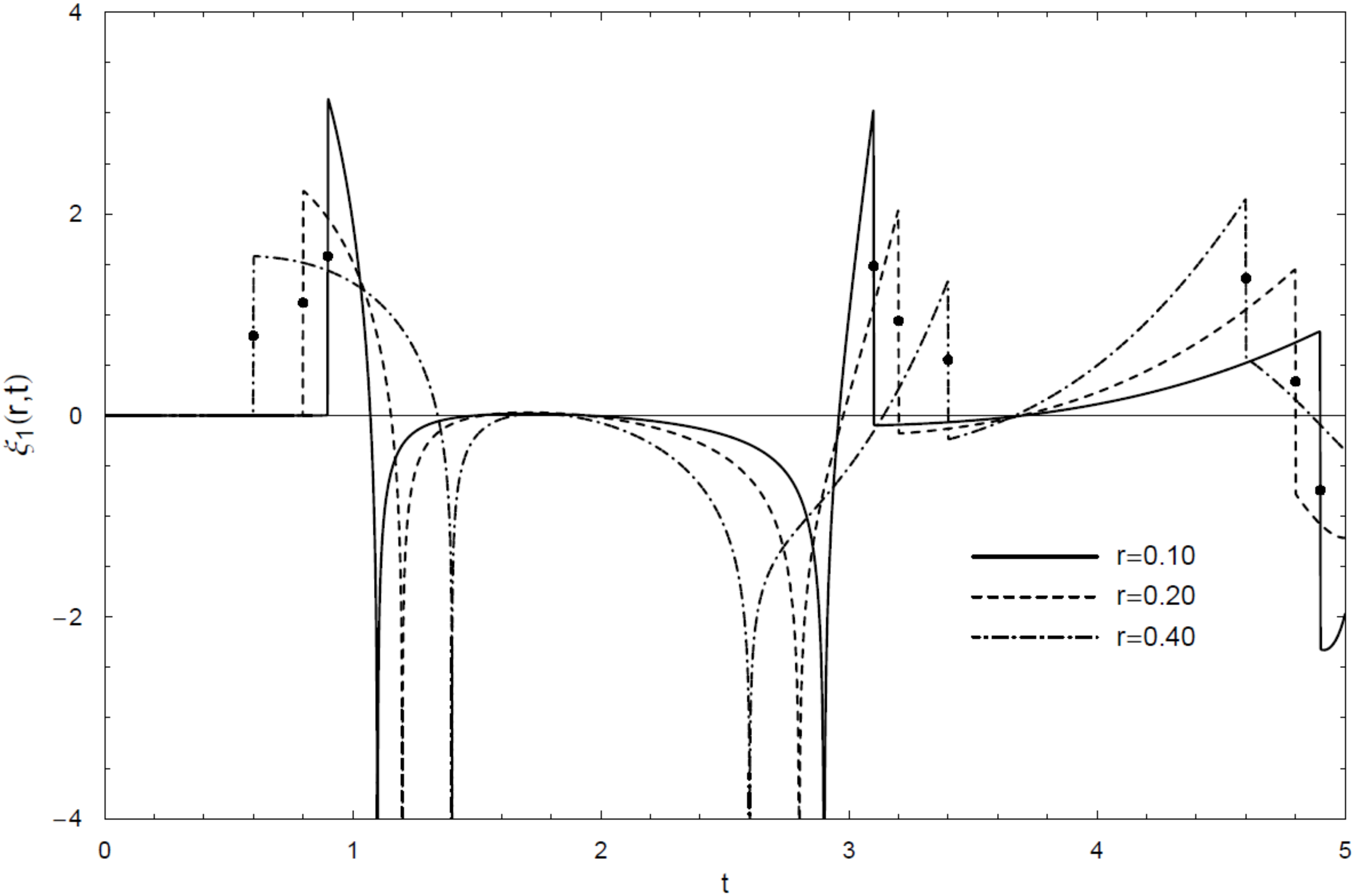

4
2
0
−2
−4
$\xi_1(r,t)$
0
1
2
3
4
5
t
r=0.10
r=0.20
r=0.40

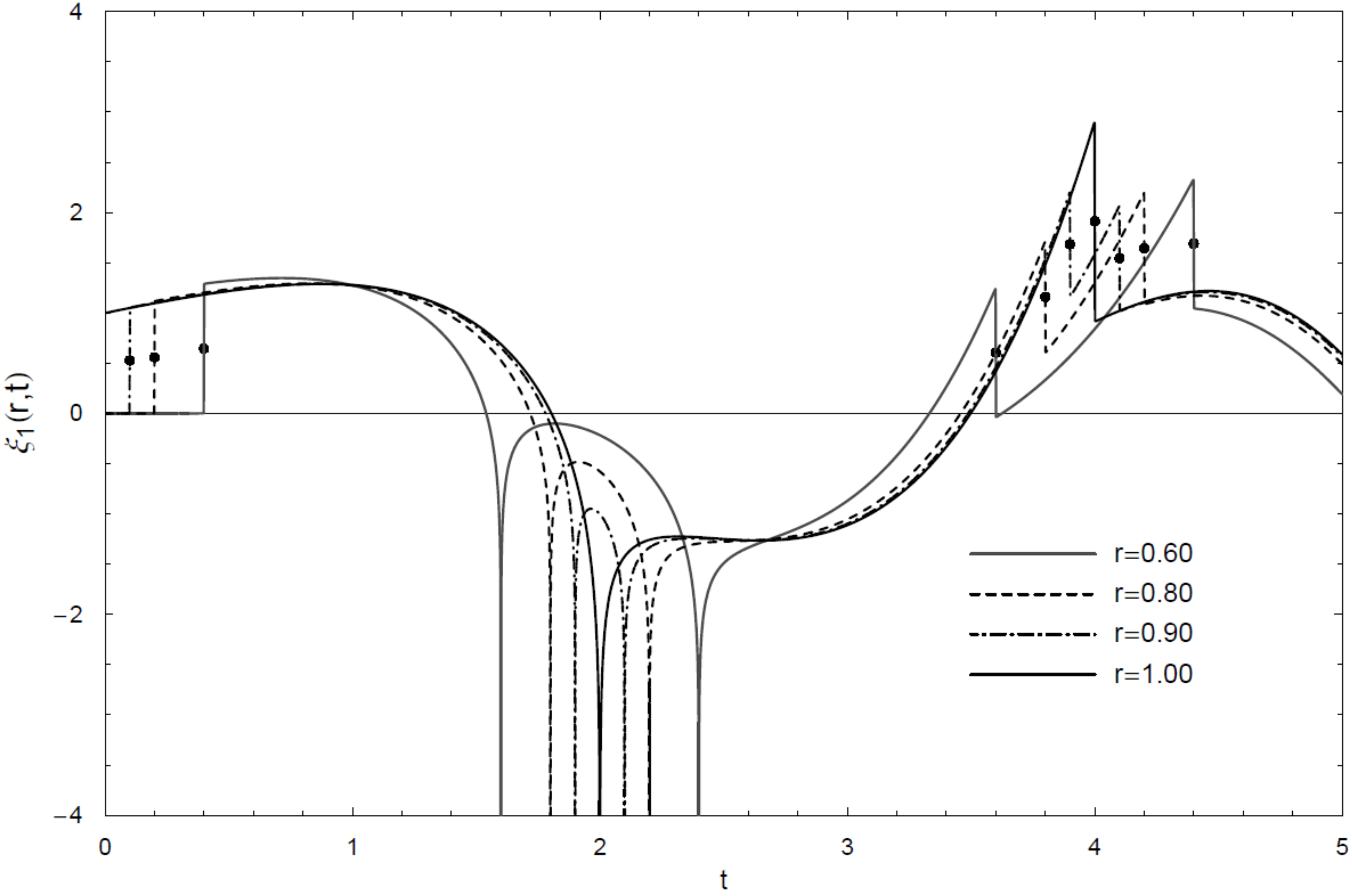

4
2
0
−2
−4
0
1
2
3
4
5
t
$\xi_1(r,t)$
r=0.60
r=0.80
r=0.90
r=1.00

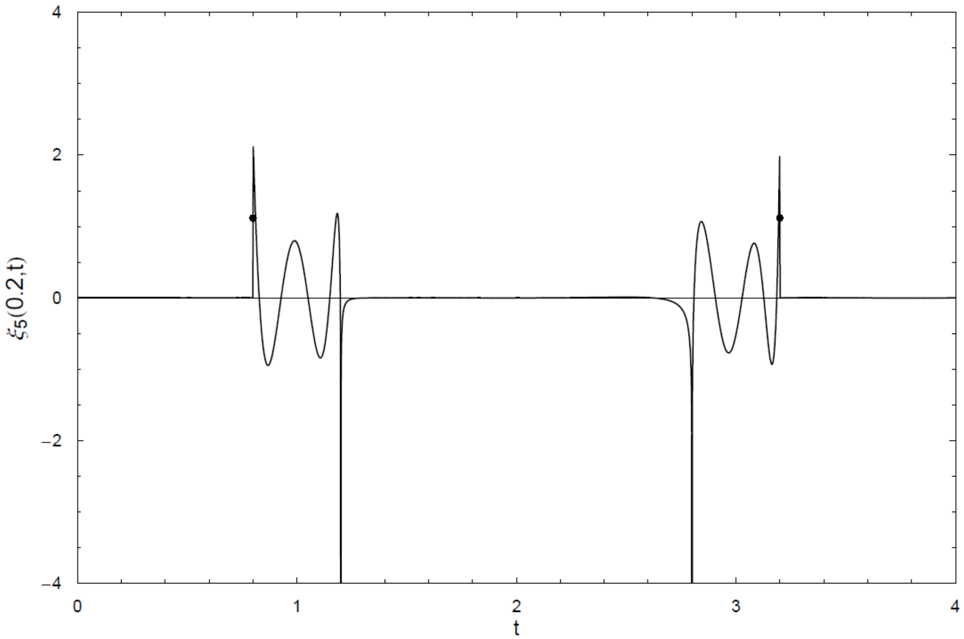

4
2
0
−2
−4
$\xi_5(0.2,t)$
0
1
2
3
4
t

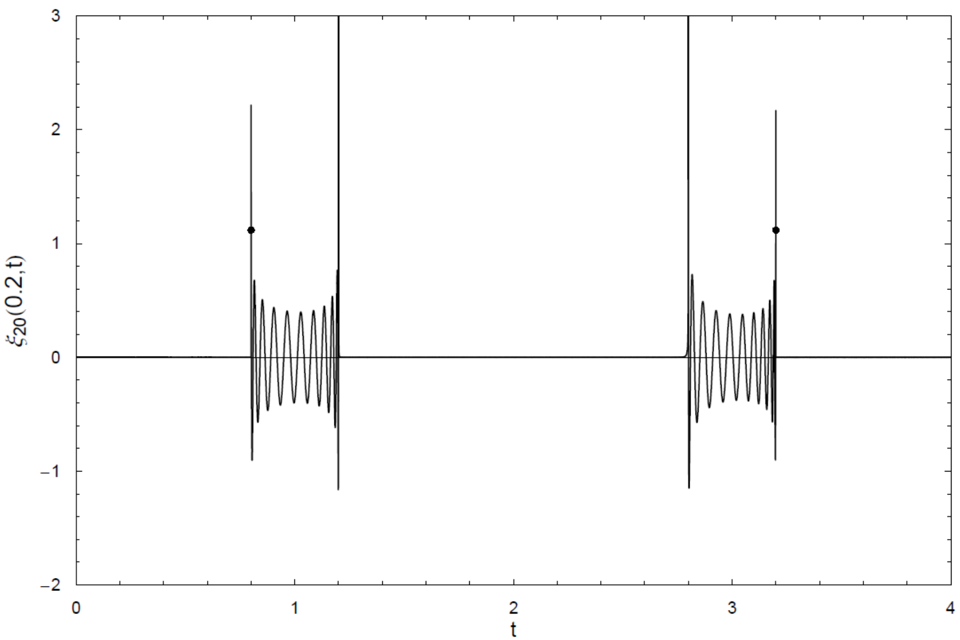

3
2
1
0
−1
−2
$\xi_{20}(0.2,t)$
0
1
2
3
4
t

Internal response functions – THE CHALLENGE

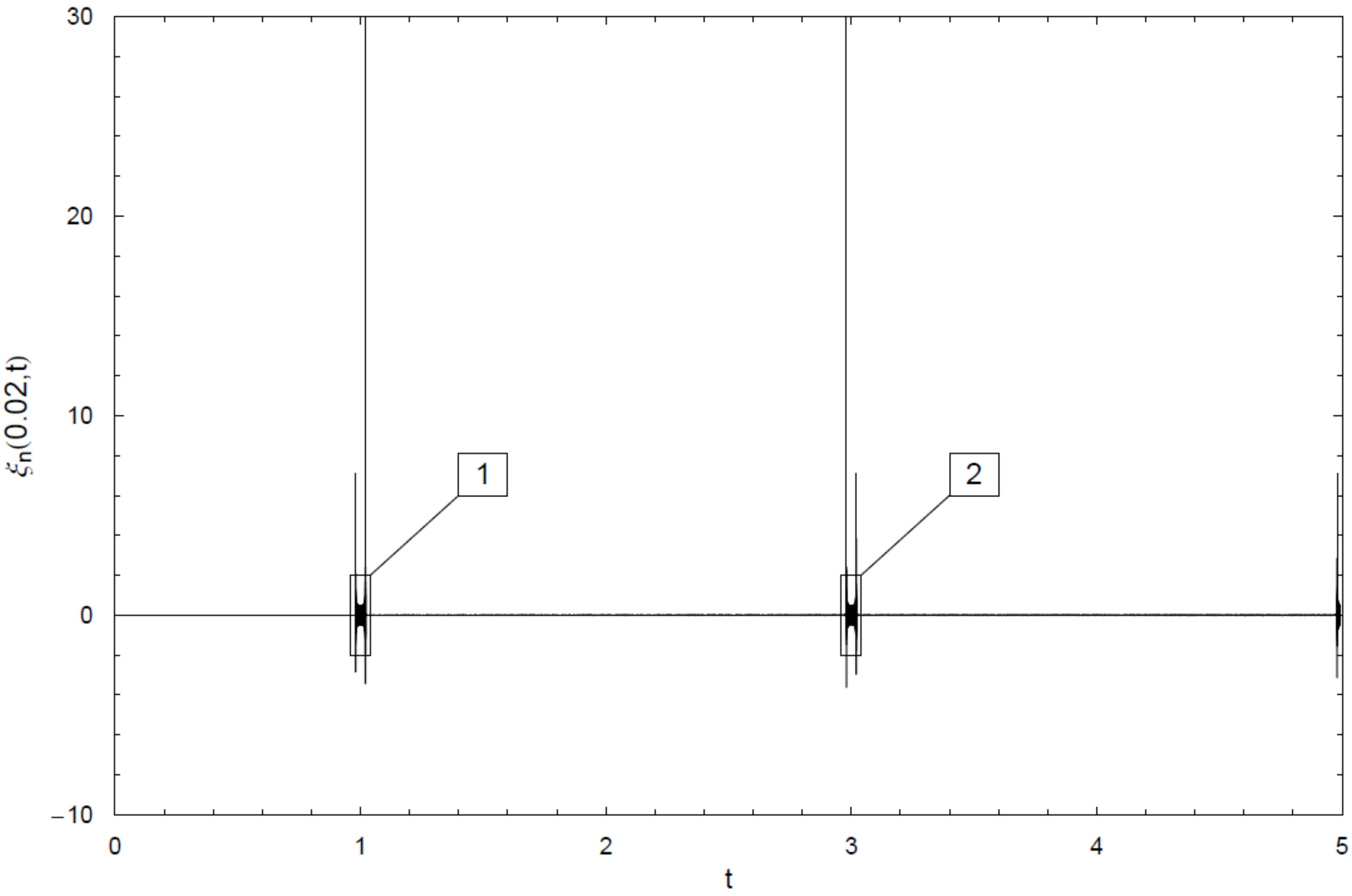

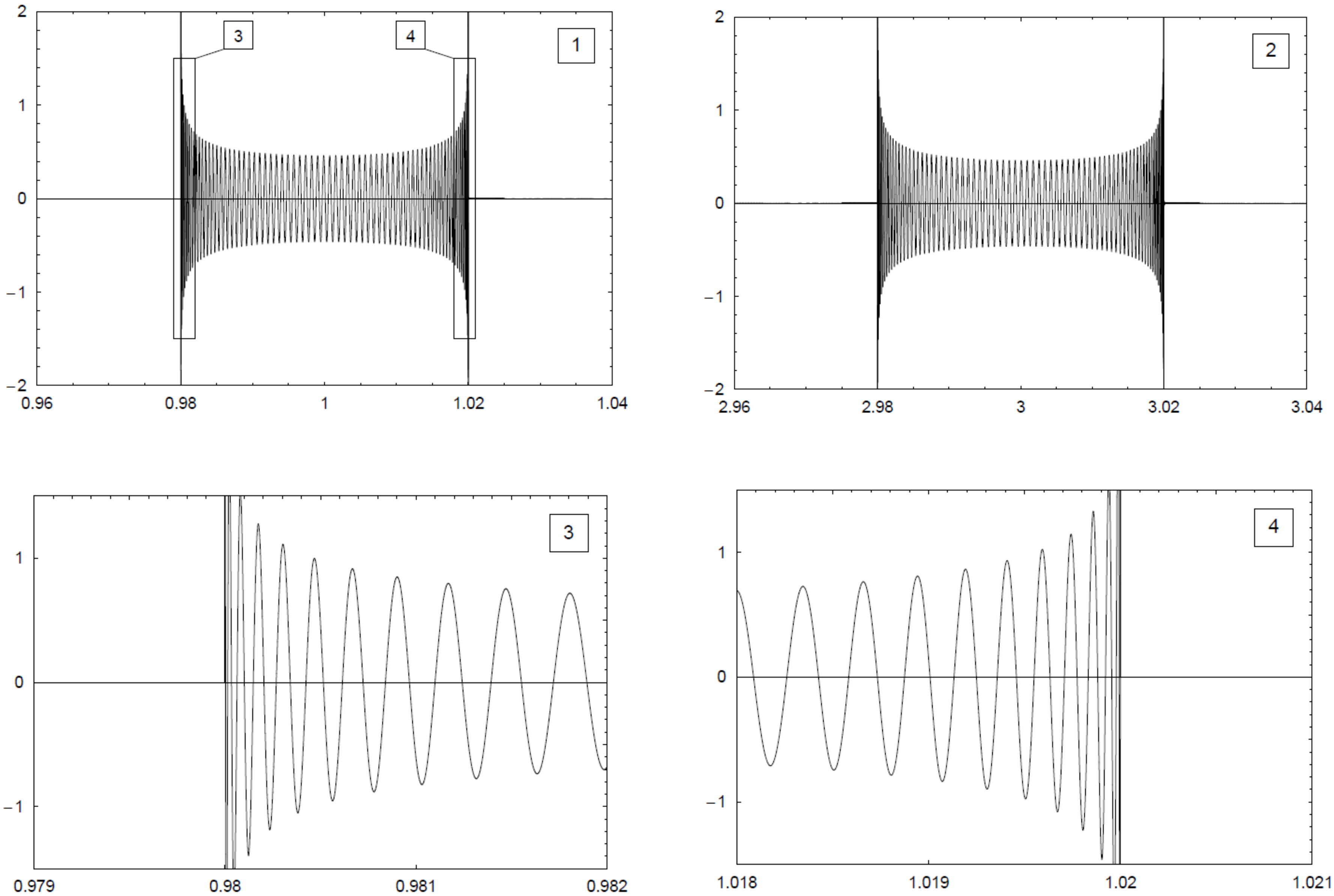

1
3
4
2
−2
−1
0
1
2
0.96
0.98
1
1.02
1.04
2.96
2.98
3
3.02
3.04
0.979
0.98
0.981
0.982
1.018
1.019
1.02
1.021

Internal shock wave propagation

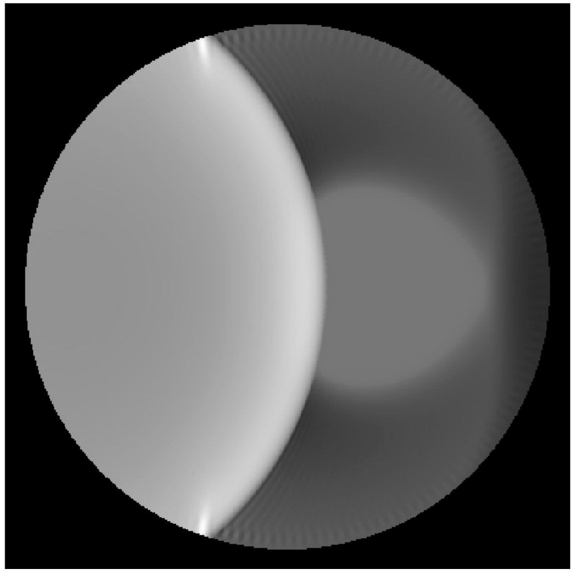

Numerically simulated pressure pattern

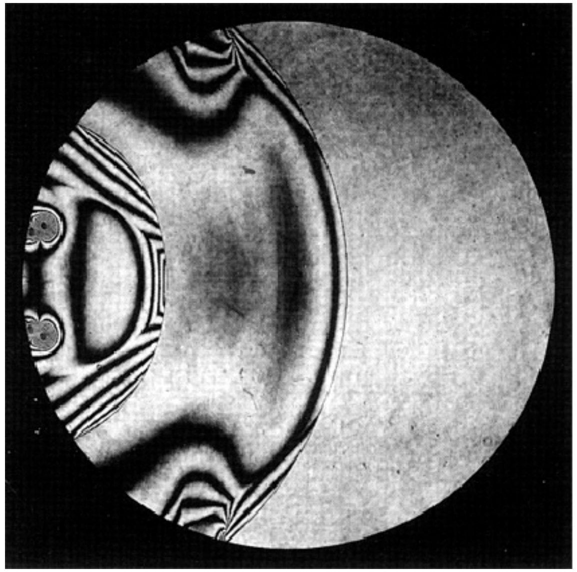

Sun, M. and Takayama, K. A holographic interferometric study of shock wave focusing in a circular reflector. *Shock Waves* 6, 1996, 323-336. © Springer Verlag.

Internal shock wave propagation

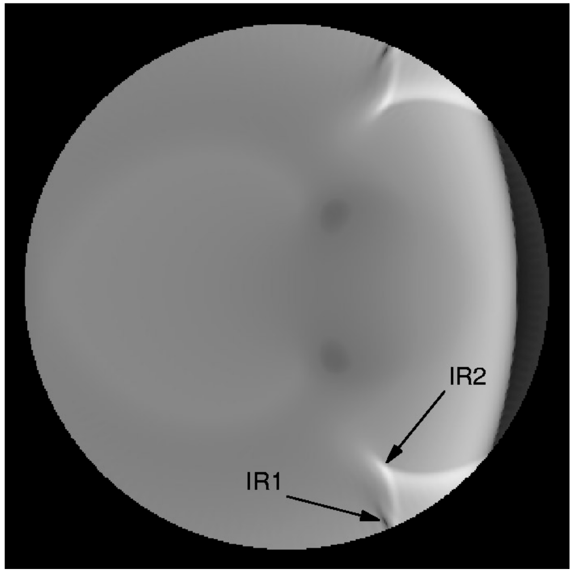

Numerically simulated pressure pattern

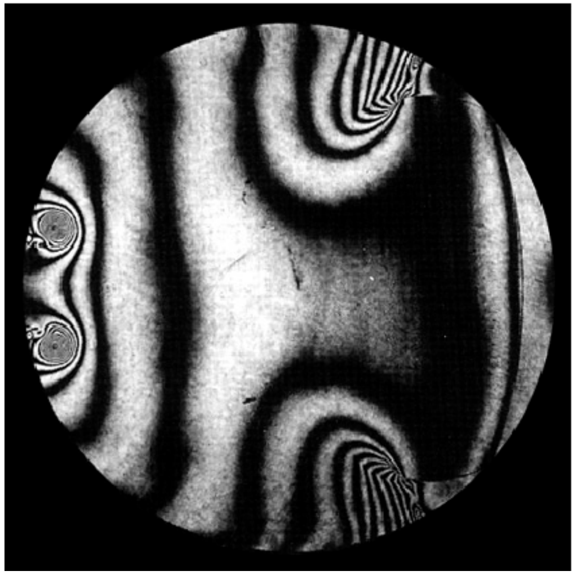

Sun, M. and Takayama, K. A holographic interferometric study of shock wave focusing in a circular reflector. *Shock Waves* 6, 1996, 323-336. © Springer Verlag.

Internal reflection

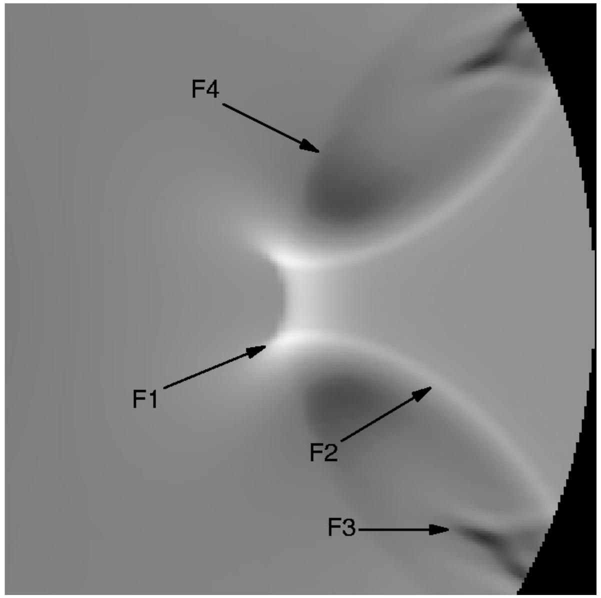

Numerically simulated pressure pattern

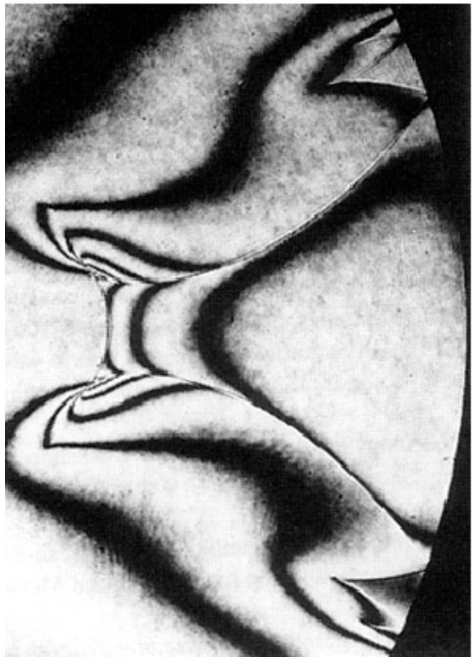

Sun, M. and Takayama, K. A holographic interferometric study of shock wave focusing in a circular reflector. *Shock Waves* 6, 1996, 323-336. © Springer Verlag.

Internal focusing

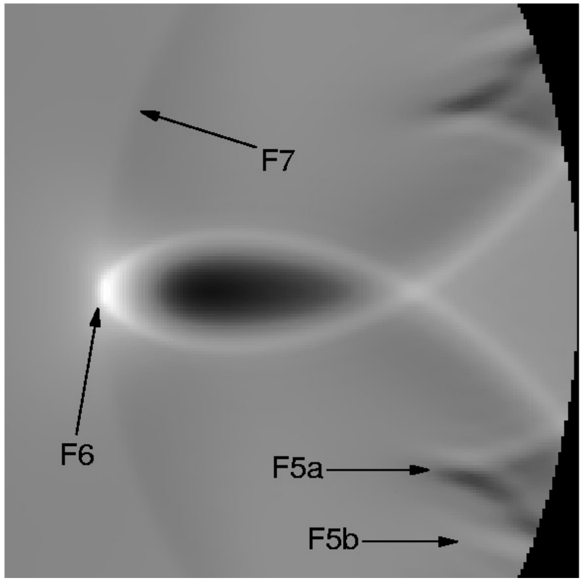

Numerically simulated pressure pattern

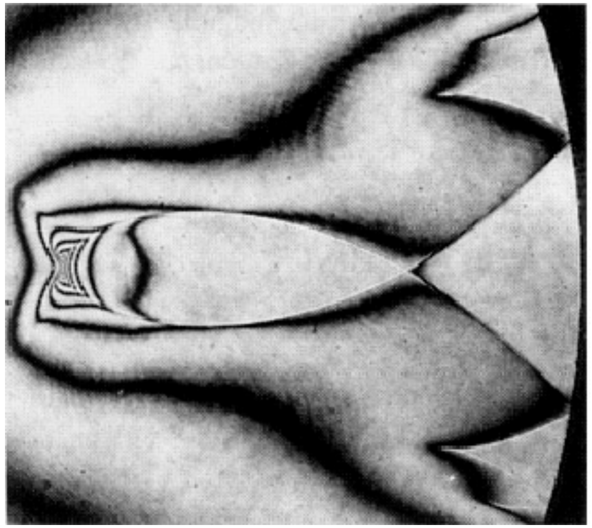

Sun, M. and Takayama, K. A holographic interferometric study of shock wave focusing in a circular reflector. *Shock Waves* 6, 1996, 323-336. © Springer Verlag.

Internal radiation pressure (qualitative comparison)

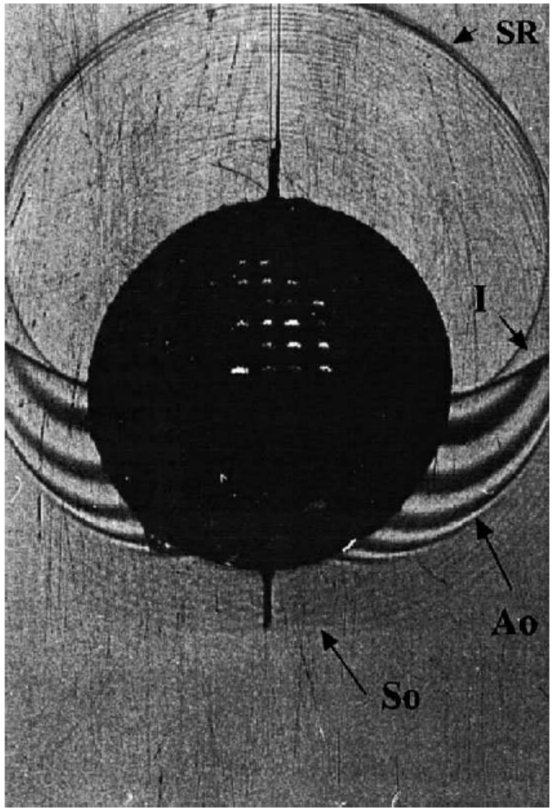

Ahyi, A. C., Pernod, P., Gatti, O., Latard, V., Merlen, A. and Uberall, H. Experimental demonstration of the pseudo-Rayleigh A0 wave. *Journal of the Acoustical Society of America* 104, 1998, 2727-2732. © American Institute of Physics.

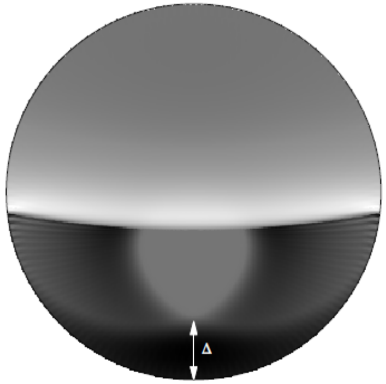

Numerically simulated pressure pattern

Late interaction – multiple regular reflection

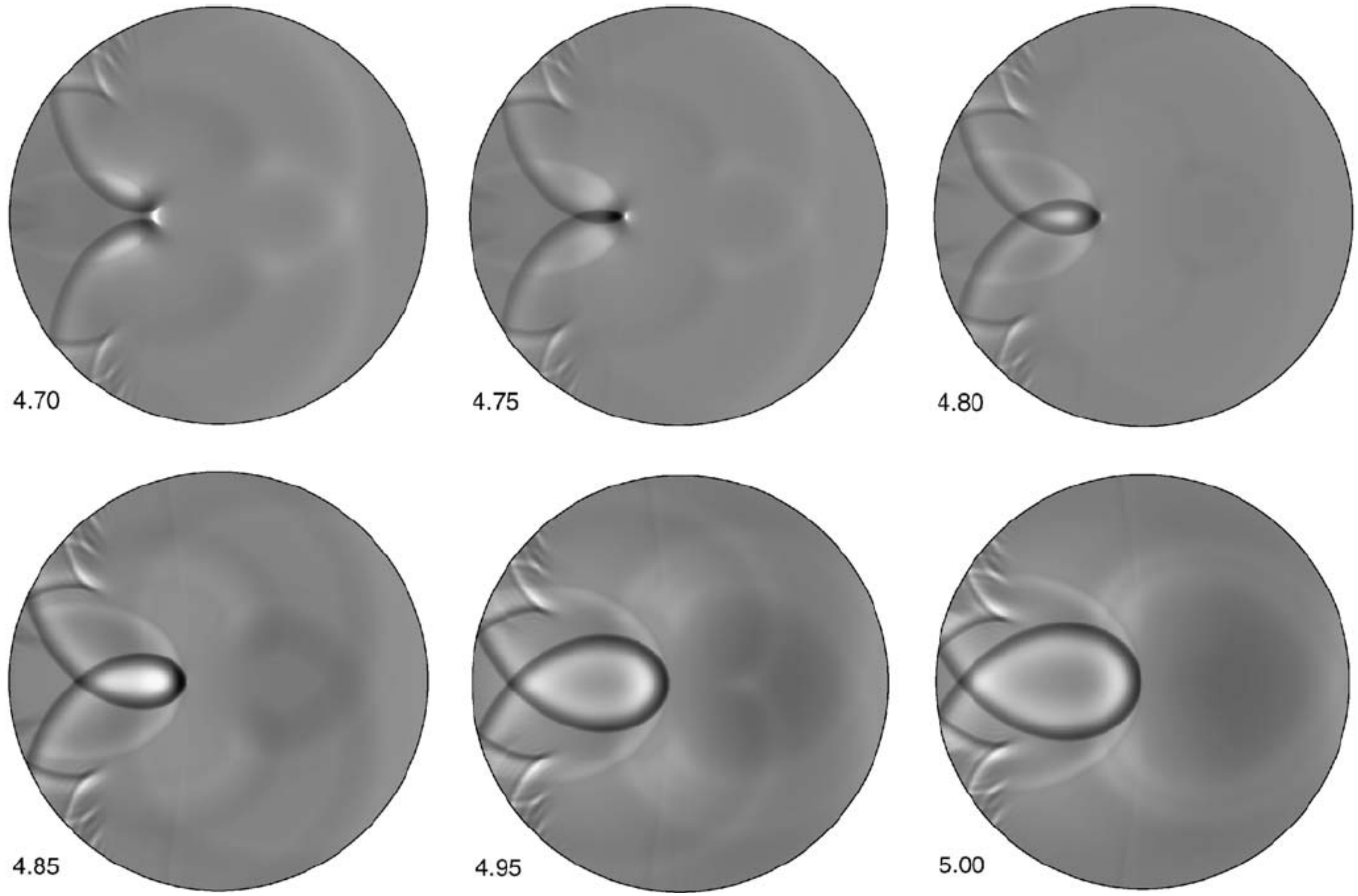

Overall dynamics

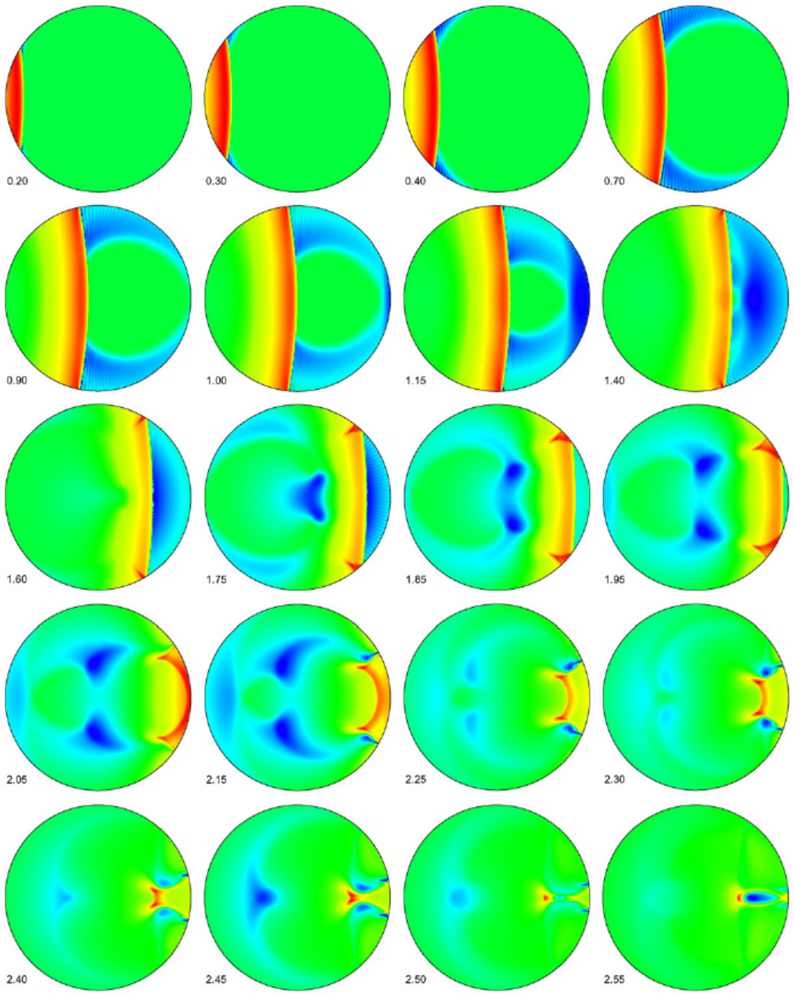

t=0.00-2.55

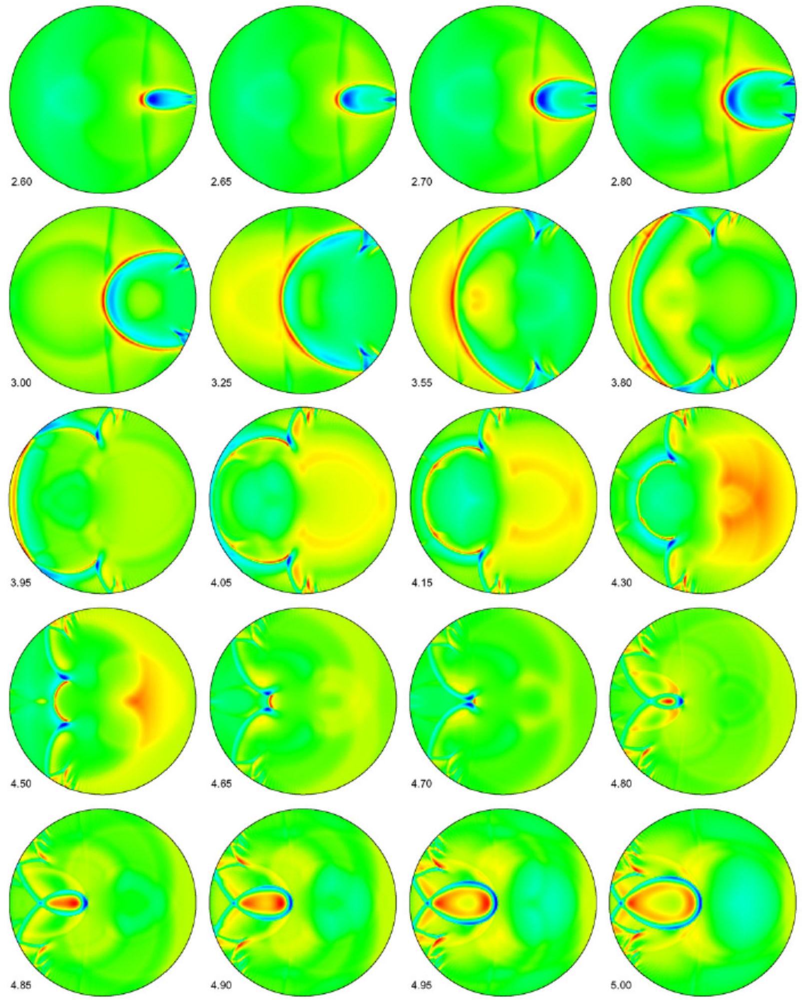

t=2.55-5.00

Part III:

Structurally enhanced shell system
(3D analysis)

Inspired by Geers (1969) and a need for
better performing fluid-interacting structures

Geometry of the problem

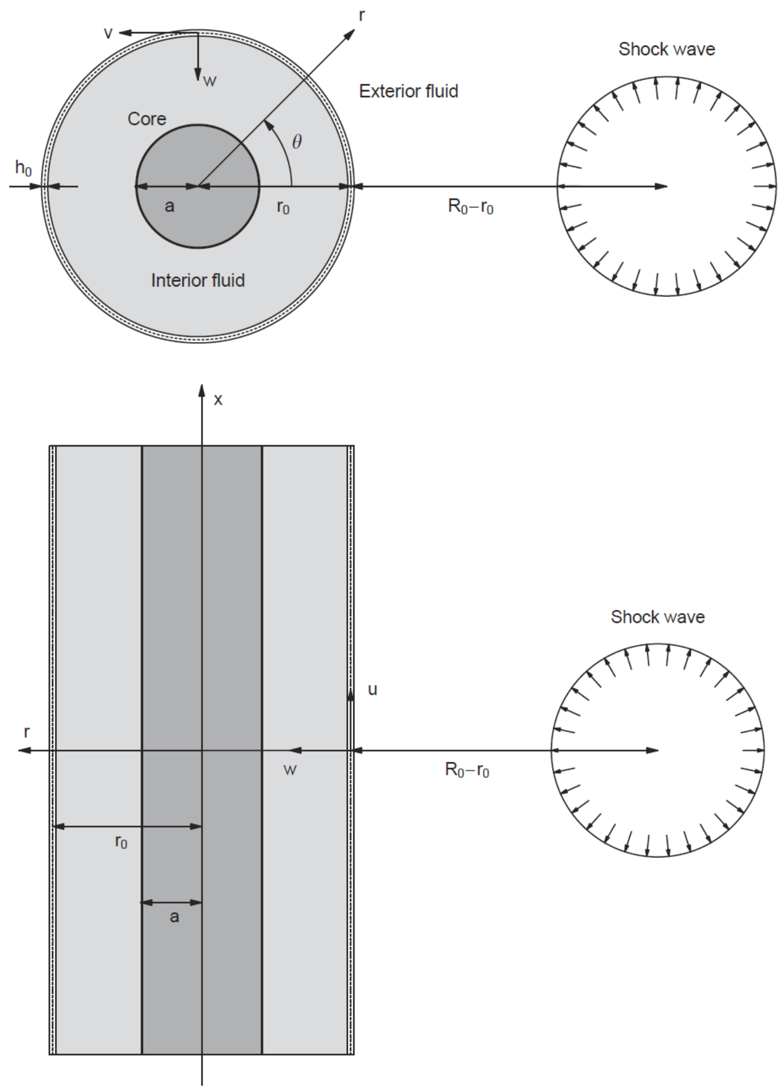

Solution – fluid dynamics

$$\frac{\partial^2 \bar{\Phi}_e}{\partial \bar{r}^2} + \frac{1}{\bar{r}} \frac{\partial \bar{\Phi}_e}{\partial \bar{r}} + \frac{\partial^2 \bar{\Phi}_e}{\partial \bar{x}^2} + \frac{1}{\bar{r}^2} \frac{\partial^2 \bar{\Phi}_e}{\partial \theta^2} - s^2 \bar{\Phi}_e = 0$$

$$\bar{\Phi}^i_{mn} = \{F_{mn} \mathrm{I}_n(\bar{r}\beta_m(s\bar{c}_i^{-1})) + G_{mn} \mathrm{K}_n(\bar{r}\beta_m(s\bar{c}_i^{-1}))\} \cos(\tilde{m}\bar{x}) \cos(n\theta)$$

Solution – fluid dynamics

$$\bar{\Phi}^{e}_{mn} = D_{mn}\mathrm{K}_n(\bar{r}\beta_m(s))\cos(\tilde{m}\bar{x})\cos(n\theta)$$

$$\bar{\Phi}^{i}_{mn} = \{F_{mn}\mathrm{I}_n(\bar{r}\beta_m(s\bar{c}_i^{-1})) + G_{mn}\mathrm{K}_n(\bar{r}\beta_m(s\bar{c}_i^{-1}))\}\cos(\tilde{m}\bar{x})\cos(n\theta)$$

$$\beta_m(s) = \sqrt{\tilde{m}^2 + s^2} \qquad \tilde{m} = (2m+1)\pi(2\bar{L})^{-1}$$

$$\bar{\Phi}^{d}_{mn} = \bar{B}_{mn}(s)\Psi^{e}_{mn}(s)\cos(\tilde{m}\bar{x})\cos(n\theta)$$

$$\bar{\Phi}^{r,e}_{mn} = s\bar{W}_{mn}(s)\Psi^{e}_{mn}(s)\cos(\tilde{m}\bar{x})\cos(n\theta)$$

$$\bar{\Phi}^{r,i}_{mn} = -s\bar{W}_{mn}(s)\Psi^{i}_{mn}(s\bar{c}_i^{-1})\cos(\tilde{m}\bar{x})\cos(n\theta)$$

$$\bar{p}^{d}_{mn}(\bar{t}) = -\bar{b}_{mn}(\bar{t}) - \int\limits_{0}^{\bar{t}} \bar{b}_{mn}(\xi) \frac{d\psi^{e}_{mn}}{d\xi}(\bar{t} - \xi)\, d\xi$$

$$\bar{p}^{r,e}_{mn}(\bar{t}) = -\int\limits_{0}^{\bar{t}} \frac{d^2 \bar{w}_{mn}(\xi)}{d\xi^2} \psi^{e}_{mn}(\bar{t} - \xi)\, d\xi$$

$$\bar{p}^{r,i}_{mn}(\bar{t}) = \bar{\rho}_i \bar{c}_i \int\limits_{0}^{\bar{t}} \frac{d^2 \bar{w}_{mn}(\xi)}{d\xi^2} \psi^{i}_{mn}\left(\bar{c}_i(\bar{t} - \xi)\right)\, d\xi$$

$$\Psi^{e}_{mn}(s) = -\frac{\mathrm{K}_n(\beta_m(s))}{\beta_m(s)\mathrm{K}'_n(\beta_m(s))}$$

$$\Psi^{i}_{mn}(s) = \frac{1}{\beta_m(s)} \frac{\{\mathrm{I}'_n(a\beta_m(s))\mathrm{K}_n(\beta_m(s)) - \mathrm{K}'_n(a\beta_m(s))\mathrm{I}_n(\beta_m(s))\}}{\{\mathrm{K}'_n(\beta_m(s))\mathrm{I}'_n(a\beta_m(s)) - \mathrm{I}'_n(\beta_m(s))\mathrm{K}'_n(a\beta_m(s))\}}$$

$$\bar{p} = \sum_{m=0}^{\infty}\sum_{n=0}^{\infty} \bar{p}_{mn}(t)\cos(\tilde{m}\bar{x})\cos(n\theta)$$

“Core” response functions

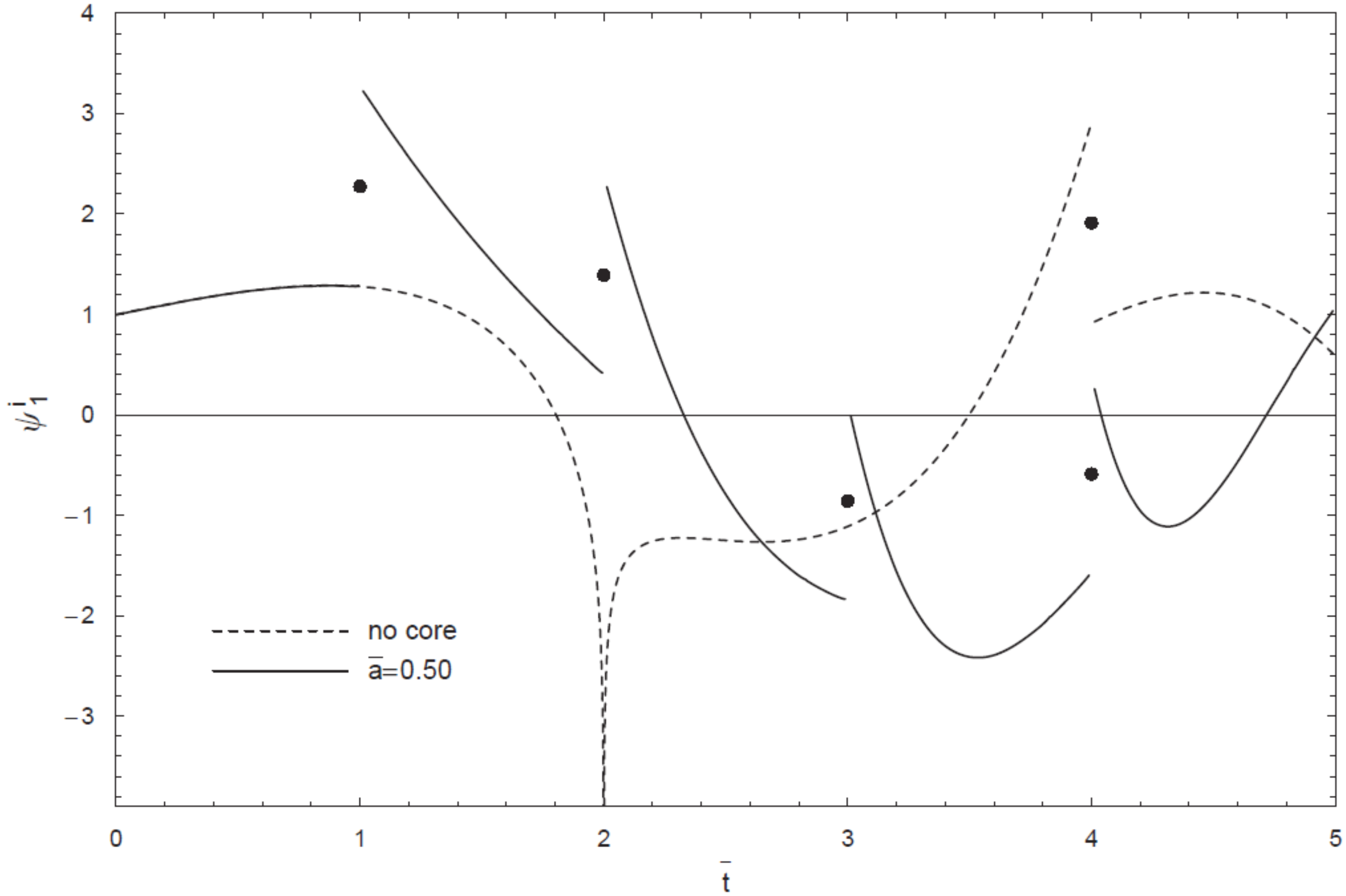

“Core” response functions

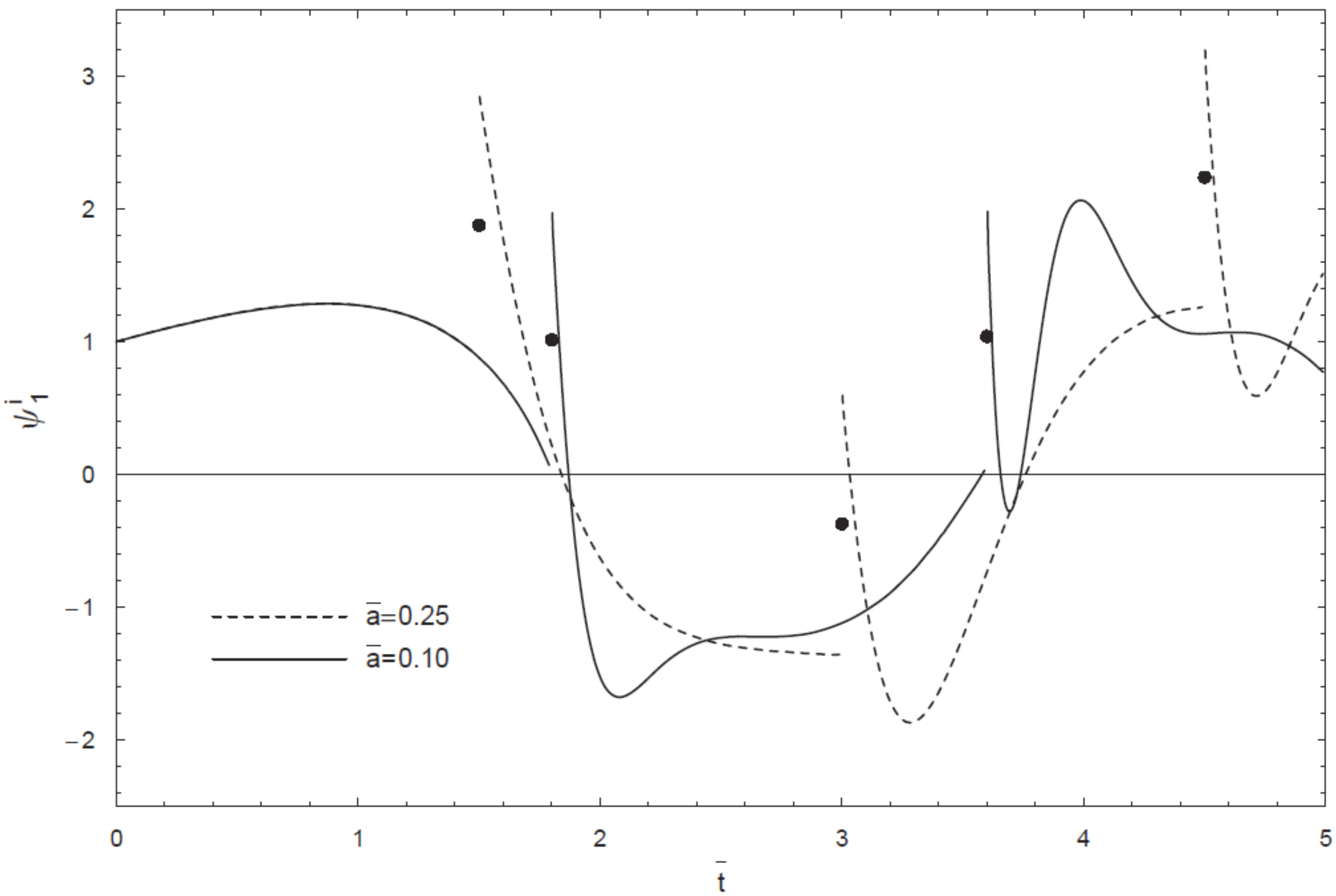

Solution – structural dynamics

$$\bar{u} = \sum_{m=0}^{\infty} \sum_{n=0}^{\infty} \bar{u}_{mn}(\bar{t}) \sin(\tilde{m}\bar{x}) \cos(n\theta),$$

$$\bar{v} = \sum_{m=0}^{\infty} \sum_{n=0}^{\infty} \bar{v}_{mn}(\bar{t}) \cos(\tilde{m}\bar{x}) \sin(n\theta),$$

$$\bar{w} = \sum_{m=0}^{\infty} \sum_{n=0}^{\infty} \bar{w}_{mn}(\bar{t}) \cos(\tilde{m}\bar{x}) \cos(n\theta)$$

Solution – structural dynamics

$$\gamma^2 \frac{\mathrm{d}^2 \bar{u}_{mn}}{\mathrm{d}\bar{t}^2} + c_{mn}^{11} \bar{u}_{mn} + c_{mn}^{12} \bar{v}_{mn} + c_{mn}^{13} \bar{w}_{mn} = 0,$$

$$\gamma^2 \frac{\mathrm{d}^2 \bar{v}_{mn}}{\mathrm{d}\bar{t}^2} + c_{mn}^{21} \bar{u}_{mn} + c_{mn}^{22} \bar{v}_{mn} + c_{mn}^{23} \bar{w}_{mn} = 0,$$

$$\gamma^2 \frac{\mathrm{d}^2 \bar{w}_{mn}}{\mathrm{d}\bar{t}^2} + c_{mn}^{31} \bar{u}_{mn} + c_{mn}^{32} \bar{v}_{mn} + c_{mn}^{33} \bar{w}_{mn} = \chi \bar{p}_{mn},$$

Deformations of the structure

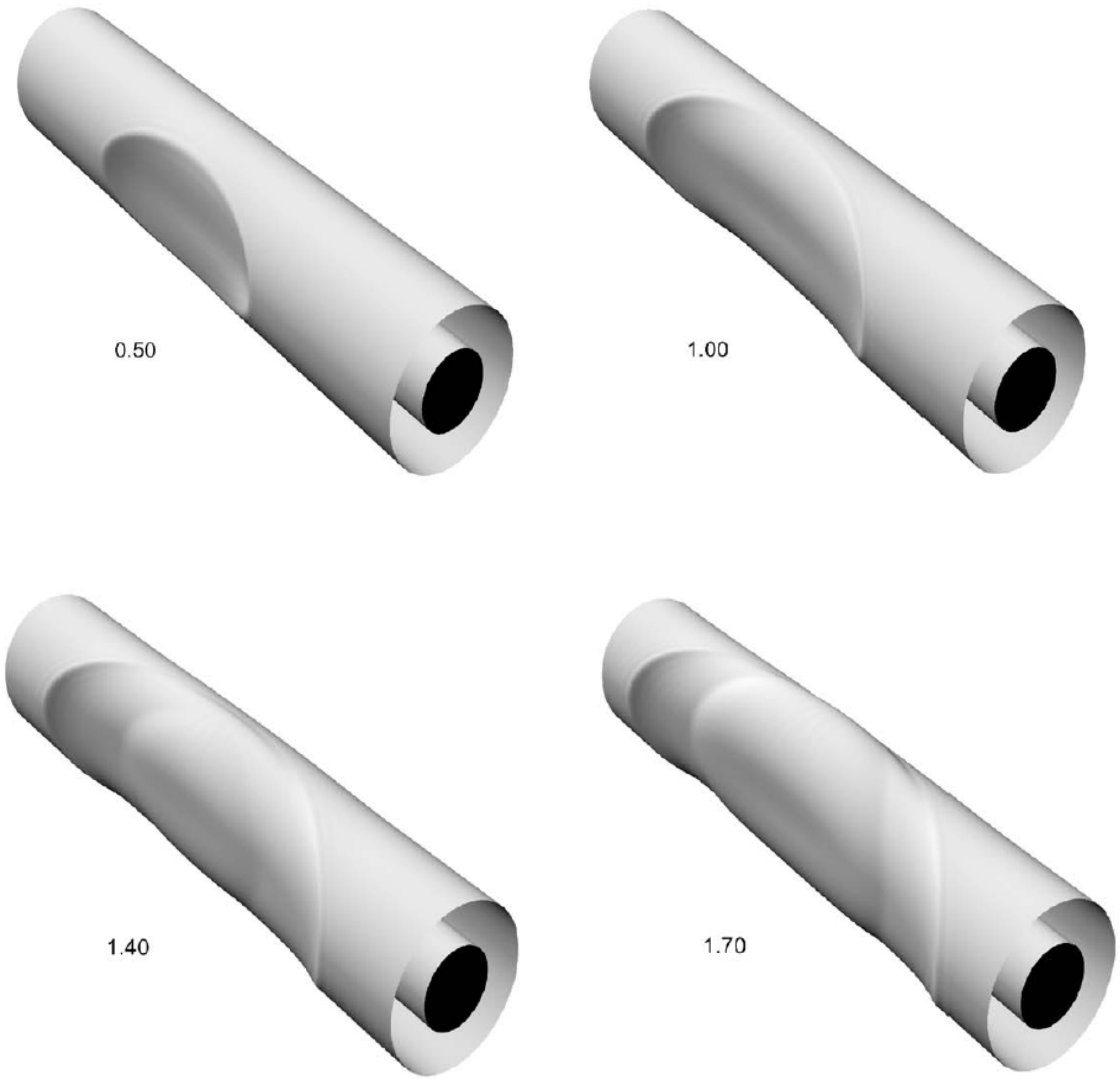

Dynamics of the stress-strain state
(core is not shown, early interaction)

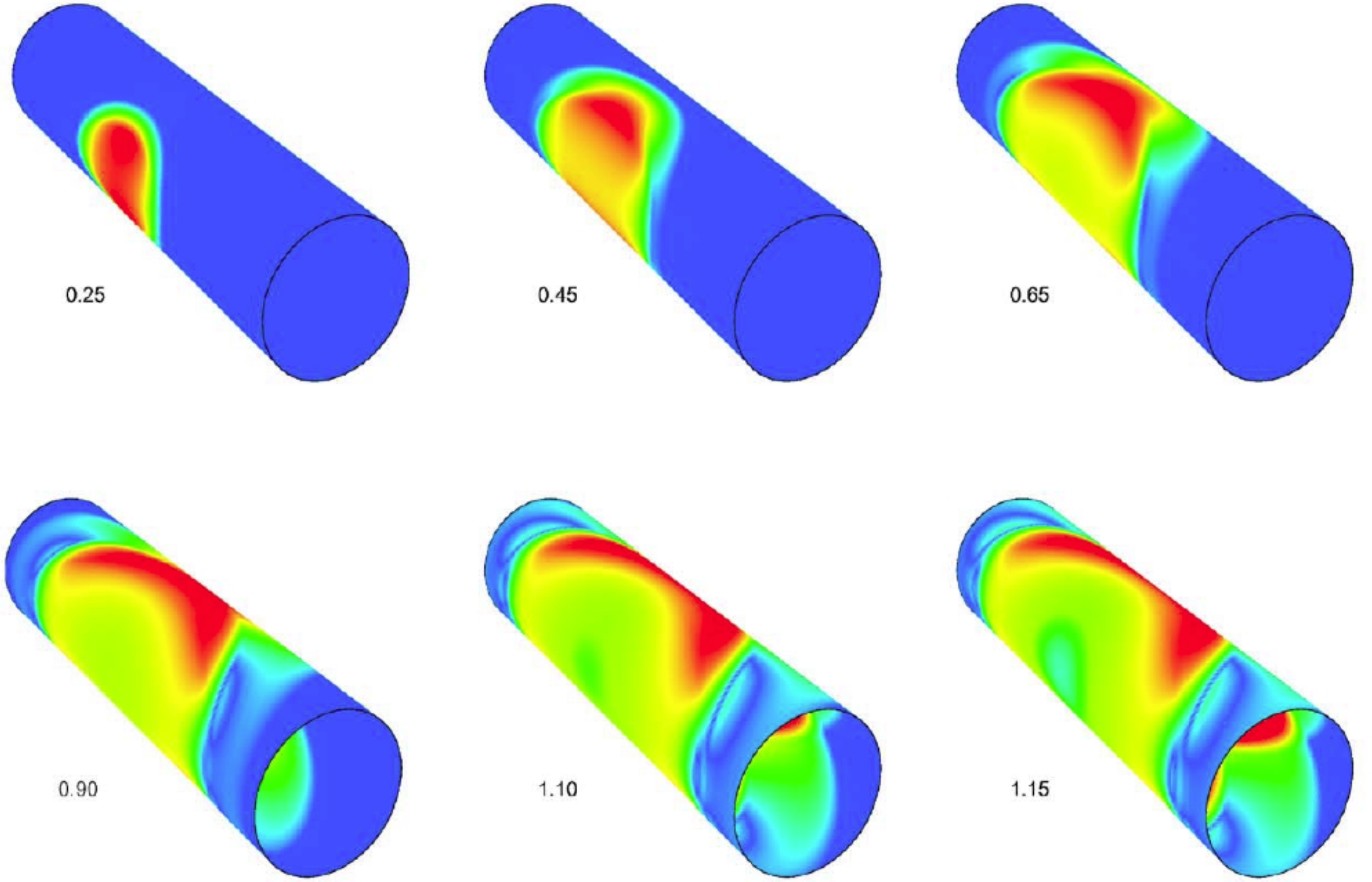

Dynamics of the stress-strain state (core is not shown, mid-interaction)

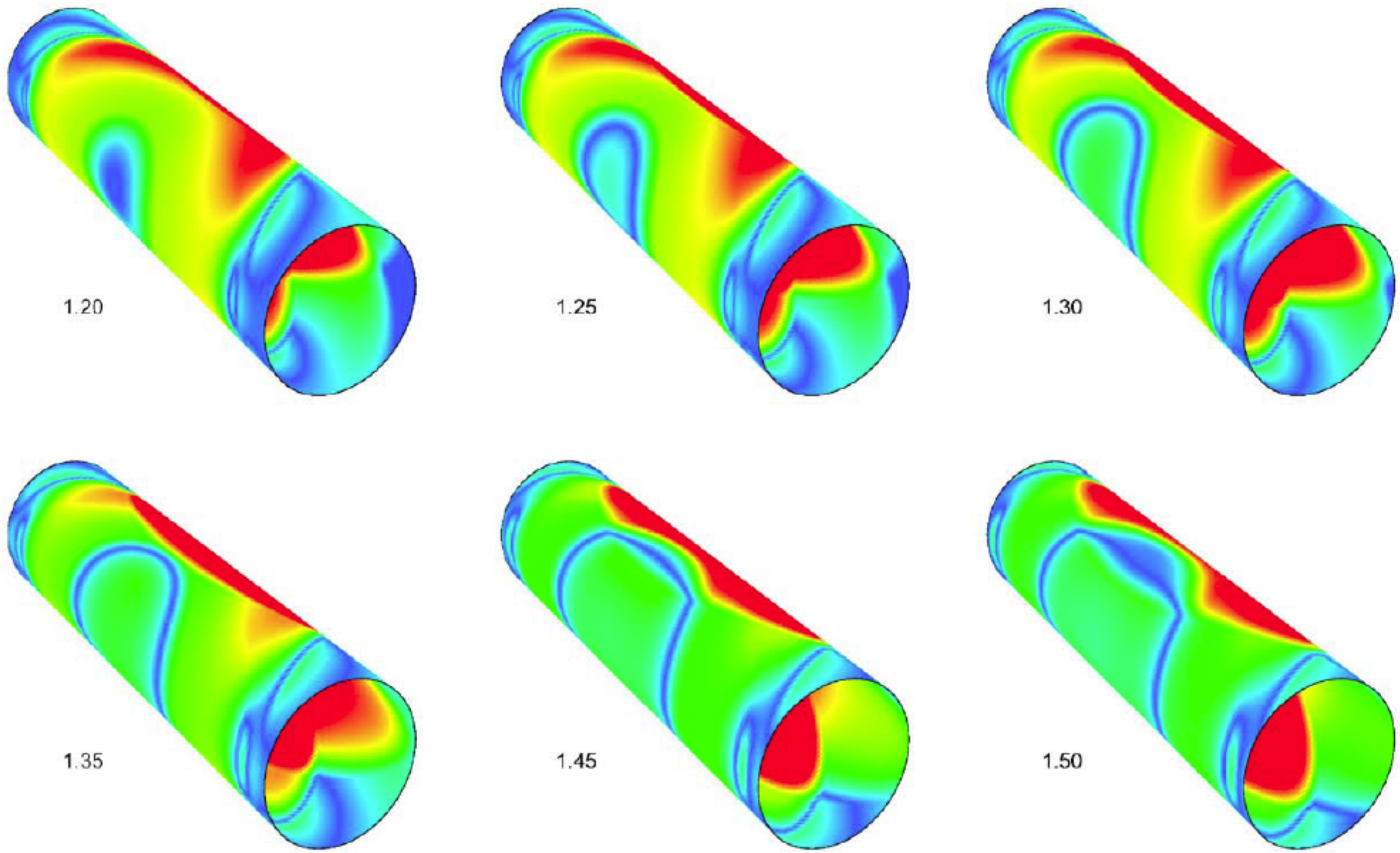

Dynamics of the stress-strain state
(core is not shown, mid-interaction)

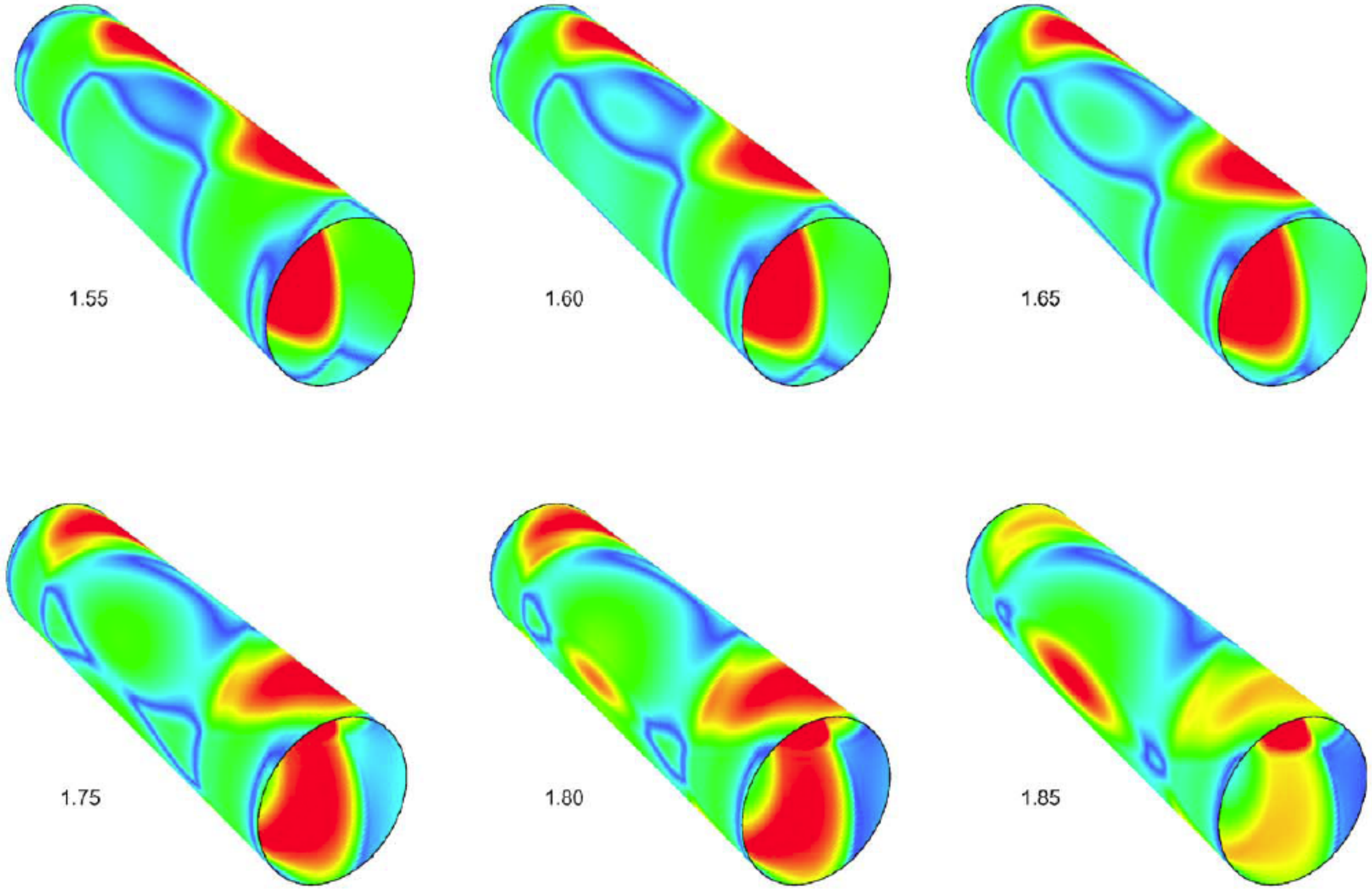

Dynamics of the stress-strain state
(core is not shown, mid-interaction)

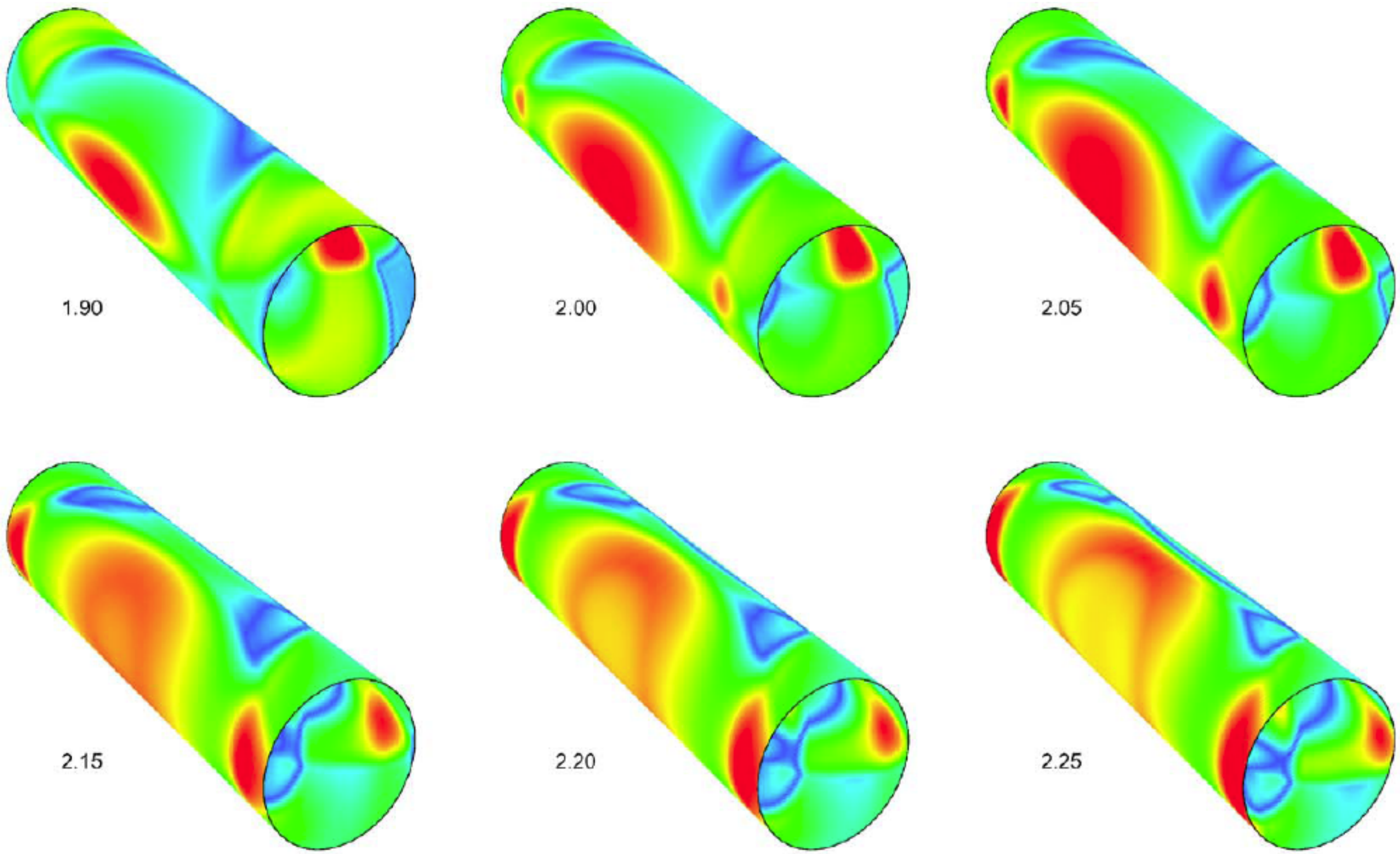

Considerable reduction of the overall tensile stress

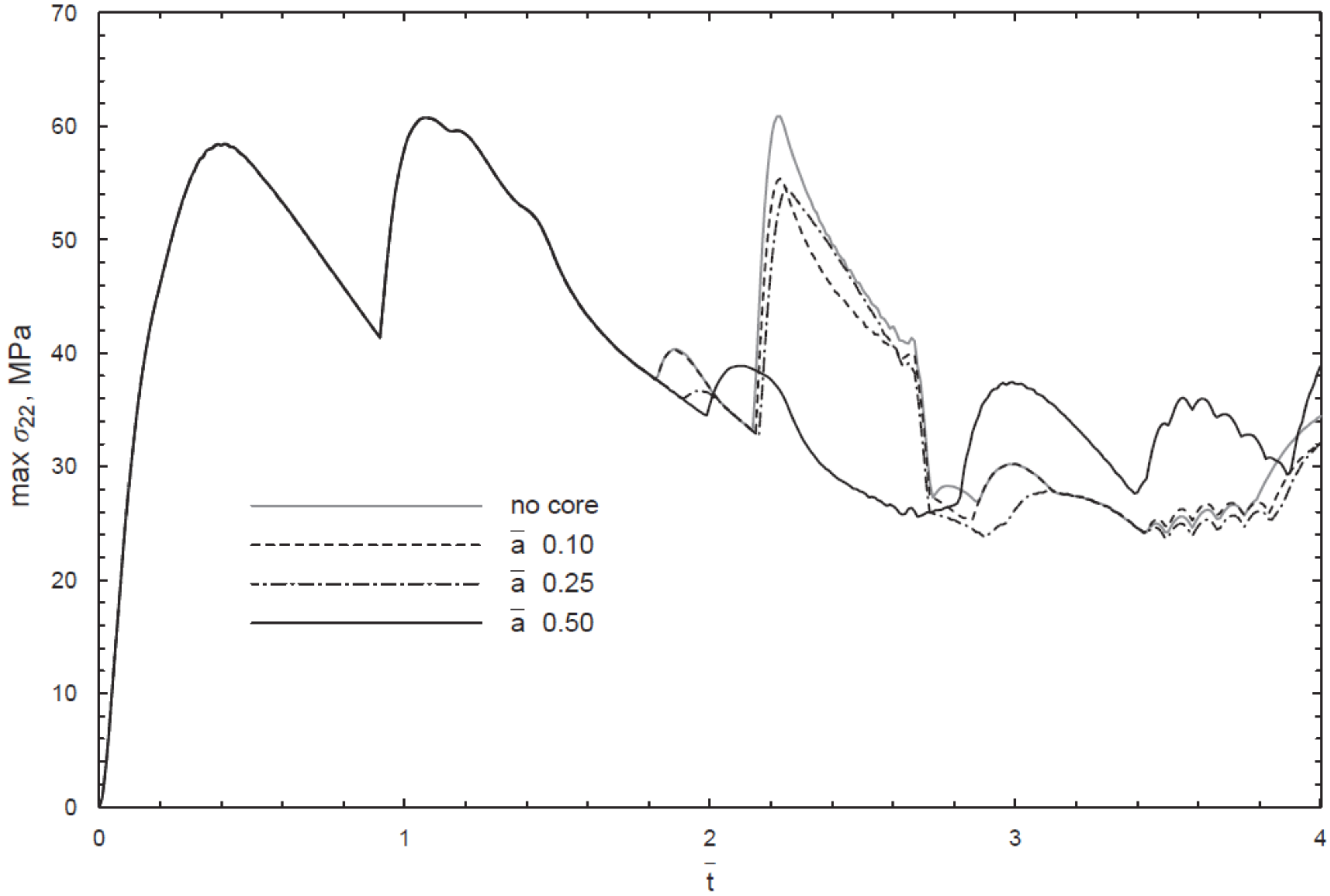

Conclusions:

classical analytical methods of mathematical physics are a valuable tool of mathematical modeling of non-stationary fluid-structure interaction when the loads are limited to acoustic pulses and very weak shock waves;

not only they provide results that excellently agree with experiments, they also allow one to gain some important insights into the physics of the problem (e.g. the response functions and analysis of structural enhancement);

the respective converged analytical solutions are an excellent source of reliable benchmarks that can be used to verify more sophisticated numerical methodologies.

Acknowledgements

This project was financially supported by the Natural Sciences and Engineering Research Council (NSERC) of Canada, the Killam Trusts, the Office of Cooperative Education at Dalhousie University and the Faculty of Engineering at Dalhousie University.

The following students have contributed to the results that were reported here:

Mathew Bligh (Mechanical Engineering, Dalhousie)
Bryan MacDonald (Mechanical Engineering , Dalhousie)
Garrett Dooley (Mechanical Engineering , Dalhousie)
Daniel Sutow (Mechanical Engineering , Dalhousie)
Martin Mitchell (Mechanical Engineering , Dalhousie)
Robynne Murray (Mechanical Engineering , Dalhousie)
Jonathan Gaudet (Proc. Eng. and Applied Science)
Kyle Williston (Environmental Engineering, Dalhousie)

Special thanks to Professor Ferdinando Auricchio and his research group (in particular, Elisa Reali and Alessandro Reali) for inviting me to spend my sabbatical leave at the Department of Structural Mechanics, and for all the support they provided with moving and settling in Pavia.